

Effects of terrestrial dissolved organic matter on a bloom of the toxic cyanobacteria, *Raphidiopsis raciborskii*

Author

Burford, MA, Franklin, H, Faggotter, SJ, Chuang, A, Hayton, JB, Carroll, AR

Published

2022

Journal Title

Harmful Algae

Version

Accepted Manuscript (AM)

DOI

[10.1016/j.hal.2022.102269](https://doi.org/10.1016/j.hal.2022.102269)

Rights statement

© 2022. This manuscript version is made available under the CC-BY-NC-ND 4.0 license <https://creativecommons.org/licenses/by-nc-nd/4.0/>

Downloaded from

<http://hdl.handle.net/10072/428999>

Griffith Research Online

<https://research-repository.griffith.edu.au>

1
2
3
4
5
6
7
8
9
10
11
12
13
14
15
16
17
18
19
20
21
22

Effects of terrestrial dissolved organic matter on a bloom of the toxic cyanobacteria, *Raphidiopsis raciborskii*

M.A. Burford^{1,2*}, H. Franklin¹, S.J. Faggotter², A. Chuang¹, J.B. Hayton², A.R. Carroll^{2,3}

¹Australian Rivers Institute, Griffith University, Nathan, Queensland, Australia

²School of Environment and Science, Griffith University, Nathan, Queensland, Australia.

³Griffith Institute for Drug Discovery, Griffith University, Nathan, Queensland, Australia

*Corresponding author:

m.burford@griffith.edu.au

23 **Abstract**

24 The concentration of coloured terrestrial dissolved organic matter (tDOM) from
25 vegetation appears to be increasing in lakes in some regions of the world, leading to
26 the term brownification. The light attenuating effect of coloured tDOM on
27 phytoplankton growth have been a major focus of attention, but the phytotoxic
28 effects of tDOM, particularly on cyanobacterial blooms, are less well understood.
29 This mesocosm study tested whether coloured tDOM, leached from the leaves of a
30 *Eucalyptus* tree species, inhibited a naturally occurring bloom of the toxic
31 cyanobacterium, *Raphidiopsis raciborskii*, in a reservoir over a 10 day period. The
32 study found that tDOM leachate, measured as dissolved organic carbon (DOC)
33 inhibited photosynthesis and growth of both *R. raciborskii*, as well as species present
34 at lower densities, i.e. other cyanobacteria and diatoms. , However, the effect was
35 greater at higher tDOM input loads. The photosynthetic yield (Fv/Fm) of
36 cyanobacteria decreased rapidly in treatments with 5.9 and 25 mg L⁻¹ DOC addition,
37 compared to the control (reservoir water with background DOC concentration of
38 6.85 ± 1.09 mg L⁻¹),. tDOM had no measurable effect in the 2 and 3.3 mg L⁻¹ DOC
39 treatments. By day 5, cell densities of cyanobacteria, including *R. raciborskii*, and
40 diatoms, in treatments with 5.9 and 25 mg L⁻¹ DOC addition were significantly lower
41 than the control with no addition, and this effect continued throughout the
42 experiment. This is despite the leachate addition increasing phosphate
43 concentrations which counteracted the low background concentrations of phosphate.
44 Light attenuation and dissolved oxygen (DO) levels were also affected by the tDOM
45 addition, but it was only significantly lower in the 25 mg L⁻¹ DOC treatment
46 compared with the control. DOC, dissolved organic nitrogen (DON) and dissolved
47 organic phosphorus (DOP) concentrations all decreased in the tDOM addition
48 treatments over the first 3 days, as the microbial cell densities increased. The
49 components of the tDOM that decreased over time were determined by ¹H NMR
50 spectroscopy in the 25 mg L⁻¹ DOC treatment. After 5 d, the relative concentrations of
51 fatty acids, sugars and gallic decreased by around 60%, while concentrations of
52 flavonoids and myo-inositol decreased by 45 and 35% respectively. This study
53 suggests that phytotoxic compounds in tDOM can suppress cyanobacterial blooms,
54 despite the increased nutrient inputs. This has implications for predicting the future
55 likelihood of cyanobacterial blooms in lakes and reservoirs with climate-change
56 driven changes in flow events and other human impacts on the amount and types of

57 vegetation cover. Revegetation of riparian zones, resulting in increased tDOM into
58 waterways, may also be beneficial in reducing cyanobacterial blooms.

59 Keywords: browning, cyanobacteria, mesocosm

60 **1. Introduction**

61 Terrestrial dissolved organic matter (tDOM) can be a major carbon input to
62 freshwater systems globally, impacting ecosystem structure and function (Prairie,
63 2008; Solomon et al., 2015). A large fraction of the tDOM is comprised of humic
64 substances that contain aromatic hydrocarbons including phenols, carboxylic acids,
65 quinones, and catechol (McDonald et al., 2004). These compounds also absorb light
66 strongly in the ultraviolet and short wavelength visible region of the spectrum, giving
67 water a brown, tea-stained colour that affects light and heat penetration (Caplanne
68 and Laurion, 2008; Fee et al., 1996; Williamson et al., 1996).

69 Studies in northern temperate and boreal areas have suggested that coloured tDOM
70 loads to lakes is increasing, a process known as browning or brownification
71 (Solomon et al., 2015; Creed et al., 2018). One compelling theory for this increased
72 load is that decreases in atmospheric sulfate deposition, as a result of emissions
73 regulations in North America and Europe, have changed soil chemistry, increasing
74 the solubility of tDOM (Monteith et al., 2007). However, many other factors, e.g.
75 wildfires, nutrient pollution and on-channel dams, can also change the quality and
76 quantity of tDOM (Xenopoulos et al., 2021).

77 Predicting the impact of an increase in tDOM on primary productivity in lakes and
78 reservoirs is challenging (Solomon et al., 2015). Much of the focus has been on the
79 light attenuating effect of coloured tDOM, reducing primary productivity through the
80 water column. This has flow-on effects such as decreasing fish production in lakes
81 (Karlsson et al., 2015). Le Bret et al., (2018) also showed that increased humic content
82 in lake mesocosms changed phytoplankton species composition towards low-light
83 adapted species, but did not affect primary productivity. Another study examined the
84 role of the microbial community in transforming tDOM in an alpine lake and inlet
85 (Stadler et al., 2020). They found that microbes were capable of thriving with tDOM
86 (= allochthonous) sources, and the positive effects on microbial growth was greater
87 than the impact of autochthonous DOM within the lake.

88 Terrestrial DOM contains nutrients, as well as organic carbon, which, in turn,
89 stimulates microbial growth. There may be trade-offs between negative effects of
90 reduced light, and positive effects of increased nutrient availability on primary
91 producers. A study of 5000 lakes globally found evidence for light/nutrient trade-offs
92 in the relationship between dissolved organic carbon (DOC) and phytoplankton

93 biomass, but this relationship varied seasonally (Isles et al., 2021). Stetler et al.,
94 (2021) analyzed data from multiple lakes to determine a positive linear relationship
95 between DOC and both total and organic forms of nitrogen and phosphorus across
96 lakes. However, analysis of long-term data from a suite of browning lakes indicated
97 that total nutrients did not increase as DOC increased through time.

98 Cyanobacteria blooms are increasing in frequency and intensity in lakes and
99 reservoirs globally, driven by increased nutrient loads and climate change (O’Neil et
100 al., 2012). Blooms have major social, environmental and economic impacts
101 (Hamilton et al., 2013). For many years, various sources of tDOM, including tDOM
102 leached from barley and rice straw, have been used to control cyanobacterial blooms
103 (Park et al., 2006; Matthijs et al., 2016). It is possible that tDOM derived from
104 catchment vegetation may have similar effects, although the evidence for growth
105 suppression on cyanobacteria and/or differential effects on cyanobacteria compared
106 with eukaryotes differed between studies (Steinberg et al., 2006; Ekvall et al., 2013;
107 Neilen et al., 2017). The growth-suppression effect is likely to be concentration-
108 dependent. Senar et al., (2021) in a study of 71 lakes, showed that low, but increasing,
109 levels of lake browning, i.e. DOC concentrations between 4 and 8 mg L⁻¹, resulted in
110 a shift from diatoms to cyanobacteria. Higher levels of lake browning, i.e. DOC
111 concentrations between 8 and 12 mg L⁻¹, resulted in a replacement of cyanobacteria
112 with mixotrophic species. Additionally, exposure time of tDOM to photochemical
113 processes can impact on the degree to which cyanobacterial growth is negatively
114 impacted (Neilen et al., 2019).

115 This mesocosm study therefore examined the impact of tDOM leached from the
116 leaves of a common tree species, *Eucalyptus tereticornis*, on a naturally occurring
117 bloom of a toxic cyanobacterial species, *Raphidiopsis raciborskii* (Wołoszyńska)
118 Aguilera, Berrendero Gómez, Kastovsky, Echenique & Salerno (basionym
119 *Cylindrospermopsis raciborskii* (Wołoszyńska) Seenayya & Subba Raju) (Aguilera et
120 al., 2018). A range of tDOM concentrations were tested to determine threshold
121 effects, and the potential role of driving factors was explored.

122

123 **2. Methods**

124 In summary, a mesocosm experiment tested the effect of tDOM (measured as
125 dissolved organic carbon (DOC)) leached from leaves of the terrestrial tree,
126 *Eucalyptus tereticornis* subsp. *tereticornis* on the growth of a naturally occurring
127 toxic cyanobacterial bloom of *R. raciborskii* (initial densities $161,917 \pm 31,164$ cells
128 mL^{-1}). The tree and cyanobacterial species were chosen to validate laboratory studies
129 testing the effect of leaf leachate on cyanobacterial photosynthesis (Neilen et al.,
130 2019; 2020). The experiment was conducted over 10 days and changes in
131 physicochemical parameters, nutrients, organic matter composition and
132 phytoplankton and bacterial measures were determined.

133 *2.1 Leaching of tDOM from Eucalyptus leaves*

134 Leaf material was collected from mature trees of *Eucalyptus tereticornis* subsp.
135 *tereticornis* (Forest Red Gum), an evergreen native Australian species widespread in
136 riparian zones of eastern Australia (Boland et al., 2006). It grows in a wide range of
137 latitudes from southern Papua New Guinea (15°S) to southeast Victoria, Australia
138 (38°S). Green leaves were collected from five individual trees on the banks of a
139 tributary of Oxley Creek, Brisbane, Australia (27°32'51.82"S, 153° 2'14.52"E) two
140 weeks prior to use and bulked together. To standardize leaf litter condition, dead
141 leaves, and those with disease or insect damage, were removed. Leaf material was
142 briefly rinsed under deionised (DI) water to remove dust and insects, patted dry and
143 oven dried at 50°C for 48 h (following Neilen et al., 2017; Franklin et al., 2020). This
144 artificially created leaf litter was used instead of fallen litter to standardize leaf
145 breakdown conditions and increase the repeatability of results.

146 To create the leachate, the dried whole leaf material was soaked in DI water at 50 g
147 dry litter per 1 L of water for 24 h at 22°C in the dark. Intact leaves and larger
148 fragments were removed by passing the leachate through a nylon mesh (500 μm).
149 Leachates were then centrifuged at 4°C (5 mins at 4000 rpm) to remove further
150 particulates and then passed through pre-combusted glass fibre filters (GF/F,
151 Whatman nominal pore size 0.7 μm) under light vacuum. Centrifuge tubes, glass
152 vacuum filtration equipment and plastic containers used to store leachates were acid
153 washed and rinsed with DI water prior to use. Due to the volume required (~130 L)
154 leachate was prepared and filtered in batches over an ~72 h period and stored at 4°C
155 while awaiting filtration and prior to application in the experiment. All batches were
156 mixed, and the leachate DOC concentration was measured (as a proxy for tDOM

157 concentration) ~48 h before addition to the mesocosms to calculate volumes
158 required to achieve target treatment concentrations. On the same day the leachate
159 was added to the mesocosms, an aliquot was set aside for the tDOM incubation
160 experiment (see Section 2.3), and another frozen at -80°C for subsequent freeze-
161 drying and characterization of organic fractions via ¹H nuclear magnetic resonance
162 (NMR) spectroscopy.

163 *2.2 Mesocosm experiment*

164 The mesocosm experiment was conducted near the dam wall in a subtropical
165 reservoir, Wyaralong reservoir in southeast Queensland (27°54'36.37"S,
166 152°52'53.21"E) in February 2019. The mesocosms consisted of 0.5 m × 0.5 m × 3 m
167 deep polyethylene bags with a total volume of approximately 800 L. They were
168 supported by 2 m × 2 m frames at the surface. Netting was placed over the tops of the
169 frames to prevent birds from disturbing the experimental apparatus. The mesocosms
170 were set up in blocks of four, with treatments randomly assigned. The design has
171 been used in previous experiments using phytoplankton blooms in reservoirs (Muhid
172 et al., 2013; Burford et al., 2014). The experiment was conducted for 10 days. On day
173 9, a storm destroyed some of the mesocosms. However, sampling was still conducted
174 for the remaining mesocosms on day 10.

175 There were six treatments (4 replicates) with increasing concentrations of added
176 dissolved organic matter (measured as DOC, see analysis method below):

- 177 1. Control (DI water added at an equivalent volume to leachate additions,
178 background DOC concentration of $6.85 \pm 1.09 \text{ mg L}^{-1}$)
- 179 2. Eucalyptus leachate (one off addition), 2 mg L^{-1} DOC added
- 180 3. Eucalyptus leachate (one off addition), 3.3 mg L^{-1} DOC added
- 181 4. Eucalyptus leachate (one off addition), 5.9 mg L^{-1} DOC added
- 182 5. Eucalyptus leachate (one off addition), 25 mg L^{-1} DOC added
- 183 6. Adjacent reservoir water (ambient)

184 At the commencement of the experiment, each mesocosm was filled with reservoir
185 water using a submersible pump pumping from 0.5 m below the surface (within the
186 surface mixed layer). Then the leachate was added 24 h later (designated day 0) at
187 relevant DOC concentrations for each treatment.

188 Sampling was conducted throughout the experiment with parameters measured and
 189 days of sampling outlined in Table 1.

190

191 *Table 1: Sampling design across experiment for all parameters*

Day of Expt.	0	1	2	3	5	7	10
Photosynthetic yield (Fv/Fm)	X	X	X	X	X	X	X
Physico-chemical probe measurements		X	X	X	X	X	X
Phytoplankton counts	X				X	X	X
Bacterial counts				X			
Chlorophyll <i>a</i> conc.		X		X	X	X	X
DOC conc.	X			X			X
Nutrient conc.	X			X			X
DOM absorbance + NMR measurements	X			X			X

192

193 At the commencement of sampling, the water column in each mesocosm was gently
 194 manually mixed with a Secchi disk. Then a 5 L subsample of water from each
 195 mesocosm was collected using a 3 m depth-integrated hose-pipe sampler. The hose-
 196 pipe sampler was rinsed with adjacent reservoir water in between sampling each
 197 mesocosm. Four replicates of depth integrated samples were also collected from the
 198 adjacent water in the reservoir, known as ‘ambient’.

199 On days outlined in Table 1, samples were taken for measurement of DOC and
 200 nutrient concentrations, tDOM characterization by ultraviolet (UV)-visible
 201 absorbance, i.e. SUVA (a measure of aromaticity measured at 254 nm), a_{350} (lignin
 202 derived phenol at 350 nm), a_{440} (gilvin measure at 440 nm) and SR (an inverse
 203 estimate of molecular weight (MW) using slopes of absorbances obtained from two
 204 regions (275– 295 nm and 350–400 nm, calculated as
 205 $\text{Slope}_{295} \text{Coefficient} / \text{Slope}_{350} \text{Coefficient}$ (Neilen et al. 2017)). tDOM was also
 206 characterized by ^1H nuclear magnetic resonance (NMR) spectroscopy. Additionally,
 207 samples were taken for measurement of photosynthetic yield (Fv/Fm),
 208 phytoplankton and bacterial counts, and chlorophyll *a* concentrations.

209 For tDOM characterization, as well as DOC and nutrients (ammonium,
210 nitrate/nitrite, total dissolved nitrogen (TDN), total dissolved phosphorus (TDP)),
211 samples were first filtered through 0.45 μm membrane filters into vials in situ, then
212 kept on ice during transport to the laboratory. Unfiltered samples were collected for
213 analysis of total nitrogen and phosphorus (TN and TP). Samples were then frozen at
214 -20°C prior to subsequent analysis of DOC and nutrient analyses, or -80°C for
215 characterization of tDOM by NMR. Samples for UV–visible absorption analyses were
216 kept at 4°C until analyzed in the laboratory on the same day.

217 Known volumes of samples were filtered onto glass fibre (GF/F, Whatman) filters in
218 situ for chlorophyll *a* analysis. Filters were then kept on ice in the dark until frozen at
219 -80°C in the laboratory. Samples for phytoplankton enumeration and identification
220 were fixed with Lugol's solution in situ on days 0, 5, 7 and 10. Samples were kept cool
221 until returned to the laboratory. Samples for bacterial enumeration were taken on
222 day 3, then fixed with 2.5% glutaraldehyde and kept at 4°C until analyzed. Samples
223 were also taken for photosynthetic yield (F_v/F_m) measurements, and kept in the
224 dark until measurements were done on the same day.

225 Physicochemical parameters (temperature, specific conductivity, dissolved oxygen,
226 pH and turbidity) were measured with a calibrated probe (HYDROLAB, Quanta,
227 Hydrolab Corporation, USA) (Table 1). Secchi depth readings were also undertaken
228 in each mesocosm. A subset of readings were done through the water column using a
229 PAR sensor (Licor) to determine the euphotic depth. In the control, 2 and 25 mg L^{-1}
230 DOC treatments (one replicate each), calibrated dissolved oxygen loggers (YSI
231 ProODO) were deployed 50 cm below the surface for 5 days to determine changes in
232 dissolved oxygen over time.

233 *2.3 tDOM incubation experiment*

234 A separate incubation experiment was conducted using the same leachate used in the
235 mesocosm experiment to determine the effect of aging on the tDOM characteristics
236 (following methods of Neilen et al., (2019)). This experiment was done by diluting
237 the leachate with DI water to avoid the complicating factors related to the in situ
238 (phytoplankton and other detritus) DOM. The concentrated tDOM was diluted to
239 match those added to the mesocosms on the day of leachate addition (2, 3.3, 5.9 and
240 25 mg L^{-1}). Dilute leachates (500 ml) were added to triplicate polystyrene tissue

241 culture flasks (Falcon® Tissue Culture Flasks, 750 cm², Vented) for each DOC
242 concentration. Control flasks were also prepared containing DI water. Flasks were
243 submerged in water baths and incubated outdoors exposed to a natural sunlight-
244 darkness cycle for 5 days. Light intensity and water temperature were monitored
245 during the incubation using a PAR 4-pi sensor (Licor, Lincoln, NE, USA) and Smart-
246 Button data logger (Smart-Button; ACR System, Surrey, Canada) respectively. Mean
247 daily water temperature was 27.9°C, daily ambient photon flux was 36 mol m⁻² d⁻¹,
248 and maximum photon flux during the day was 1648 μmol m⁻² s⁻¹ (2 pi sensor).
249 Previously Neilen et al., (2019) found these polystyrene flasks did not interfere with
250 light intensity. Sub-samples were collected for analysis of DOC concentrations, and
251 tDOM characterization by UV-visible absorption and NMR (only 25 mg L⁻¹ DOC
252 treatment) on day 0, and after aging for 5 days.

253 *2.4 Laboratory analyses*

254 Samples for phosphate, ammonium, nitrate + nitrite concentrations were analyzed
255 using a Discrete Chemistry Analyzer (SmartChem 200, WESTCO Scientific
256 Instruments Inc., Brookfield) (American Public Health Association (APHA), 2005).
257 TDN and TDP samples were digested using a simultaneous persulfate digestion
258 method for nitrogen and phosphorus (Hosomi and Sudo, 1986) before being
259 analyzed on the flow injection analyzer (LACHAT 8000QC). Particulate phosphorus
260 (PP) and nitrogen (PN) were determined by subtracting TDP and TDN from TP and
261 TN respectively. Dissolved organic phosphorus (DOP) was determined by subtracting
262 the inorganic form of P (phosphate) from TDP. Dissolved organic nitrogen (DON)
263 was determined by subtracting the inorganic forms of nitrogen (ammonium, nitrate
264 + nitrite) from TDN. Molar ratios were calculated for TN and TP, and compared with
265 Redfield (1958) ratio for balanced growth, i.e. 16:1, using the Isles (2020) logarithmic
266 transformation, i.e. 1.2.

267 Spectroscopic characteristics were measured on fresh samples, kept at room
268 temperature, from each mesocosm. This included UV-visible absorbance (Shimadzu
269 UV-2450 Spectrophotometer, Kyoto, Japan) following on from Helms et al., (2008),
270 and a range of spectroscopic indices to infer tDOM composition. Absorbance spectra
271 were recorded over the 290 to 750 nm wavelength range, and at 1 nm intervals.
272 Absorption coefficients (a_g m⁻¹) at 350 nm (a_{350}) were a proxy for lignin phenol

273 concentrations (Benner and Kaiser, 2011), and 440 nm (a₄₄₀) indicated gilvin
274 content (water colour due to DOM) (McDonald et al., 2004). Specific UV absorbance
275 at 254 nm (SUVA₂₅₄; L mg⁻¹ m⁻¹) was an indicator of DOC aromaticity (Helms et al.,
276 2008). The ratio of slopes (SR) for log-transformed spectral ranges of 275–295 and
277 350–400 nm was used as a metric that is negatively correlated with DOM molecular
278 weight (Yamashita et al., 2010).

279 Proton (¹H) and 2-dimensional (2-D) nuclear magnetic resonance (NMR)
280 spectroscopy were conducted on freeze-dried tDOM samples from the mesocosms
281 (25 mg L⁻¹ DOC treatment only), as well as the tDOM incubation experiment, and
282 concentrated *Eucalyptus* leachate to provide additional structural resolution and
283 quantification of tDOM components. All NMR analyses were acquired in the solvent,
284 DMSO-*d*₆ at 25 °C. Solution-state ¹H, and 2-D NMR experiments were used to
285 determine the chemical structures of compounds in the tDOM pool, and the relative
286 proportions of these compounds were quantified (see Franklin et al., 2020; 2021 for
287 further details). Few compounds in the mesocosm samples (control and 25 mg L⁻¹
288 treatments analyzed) were detected in sufficient concentrations to quantify. Where
289 signals were present in the ¹H-NMR spectra, the signal was often broad and obscured
290 quantification of individual compounds. For the tDOM incubation experiment
291 samples peaks associated with five specific compounds or compound classes were
292 identified and quantified: β-glucose, myo-inositol, fatty acids, gallic acid and
293 flavonoids. Peaks were integrated and standardized to the peak intensity of the
294 residual proton signal in the d₆-DMSO in order to compare relative molar
295 proportions quantitatively between samples. Relative molar proportions of each
296 compound group were calculated by multiplying the integral value by the sample
297 volume.

298 Due to the complexity of signals within the ¹H NMR spectra for the concentrated
299 (crude) *Eucalyptus* leachate (Fig. S1), additional identification of compounds was
300 facilitated by high-performance liquid chromatography (HPLC) separation (see
301 Supplementary Information for detailed methods). Identification of compounds in
302 the concentrated *Eucalyptus* leachate and within tDOM fractions was based on the
303 analysis of 1 and 2D NMR data (COSY, HSQC and HMBC), and validated with data
304 from the literature (e.g. Neilen et al., 2020).

305 Chlorophyll *a* concentrations were determined spectrophotometrically by sonicating
306 the glass fibre filters in 90% acetone on ice to extract the pigments. The sonicated
307 extracts were kept at -20 °C for 24 h to ensure all pigments had eluted into the
308 acetone. After this time, the samples were spun in a desktop centrifuge for 5 min at
309 800 g (~2,000 rpm; Eppendorf, Germany), filtered through glass fibre filters
310 (ADVANTEC, GF75) to remove any particulates, then absorbances were measured on
311 a spectrophotometer (Shimadzu UV-2450 Spectrophotometer, Kyoto, Japan) at 750,
312 665, 664, 647 and 630 nm (Jeffrey and Welshmeyer, 1997). Hydrochloric acid was
313 also added, and samples re-measured to determine phaeopigment concentrations for
314 subtraction from values measured from sample pre-acidification.

315 Enumeration of *R. raciborskii* and total cell counts were conducted microscopically
316 using a Sedgewick Rafter cell under a compound microscope (LEICA ICC50) with
317 400× magnification (Woelkerling, et al., 1976). Enumeration ceased after counting a
318 minimum of 23 units (trichomes/filaments or colonies), or until the average and
319 standard deviation of counts per square is stable. A minimum of 23 algal units for the
320 most abundant taxa was used to gain a precision error of ±30% (Burford et al. 2014).

321 The total algae and *R. raciborskii* biovolumes for the common phytoplankton species
322 in the study were calculated using data from an adjacent reservoir where cell
323 dimensions had been measured for multiple cells (A. Chuang, unpubl. Data), and the
324 average biovolume calculated using published equations (Hillebrand, et al., 1999).

325 Enumeration of bacteria was conducted by first staining with SYBR Gold stain
326 technique followed by epifluorescence microscope (LEICA DM 4000) at 1,000x
327 magnification (Chen et al., 2001). Enumeration ceased after a minimum of 10 field of
328 views or at least 500 bacteria were counted.

329 For measurements of photosynthetic yield (F_v/F_m), samples were dark adapted for
330 20 min prior to reading F_v/F_m using a using a PHYTO-PAM System II Emitter-
331 Detector (PHYTO-ED) unit (Heinz Walz GmbH, 2003) with PHYTO-WIN software
332 version 2.10. Duplicate measurements were made for each sub-sample.

333 *2.5 Statistical analyses*

334 All summarized data is expressed as mean ± standard deviation. The effect of each
335 mesocosm treatment on individual parameters was analyzed for data from each
336 experimental day separately using the non-parametric statistics due to non-

337 normality of much of the data. Data from each day for each treatment (plus ambient
338 water) were compared using the Kruskal-Wallis test followed by Dunn's post hoc
339 tests with Bonferroni adjustment to assess significant differences between all
340 treatment groups. The effect of each treatment and aging (raw and aged for 5 days)
341 on tDOM composition (UV-visible spectroscopic properties and compounds
342 quantified by NMR) was compared using two-way analysis of variance (ANOVA).
343 When a significant treatment effect was detected, mean estimates were compared
344 using Tukey's post-hoc tests. All statistics were performed in R version 4.0.0 (R
345 Development Core Team, 2010; Vienna, Austria, <http://www.r-project.org/>).

346 **3. Results**

347 *3.1 Mesocosm experiment*

348 3.1.1 Composition of tDOM in *Eucalyptus* leachate

349 Analysis of the ¹H NMR of fractions generated from HPLC (complemented by 2-D
350 NMR techniques) suggested the *Eucalyptus* leachate contained a wide range of
351 compound classes; with resonances consistent with phenolic, olefinic, glycosidic or
352 aliphatic bonds being prominent (see Supplementary Information, Figure S1-3, Table
353 S1). The *Eucalyptus* leachate contained sugars (α - and β -Glucose), products of
354 microbial degradation of these sugars (i.e. myo-inositol), as well as 2,3-butanediol.
355 The bulk of material that eluted directly from C₁₈ HPLC column in water prior to
356 fractionation was myo-inositol. A small proportion of phenolic (tannins) and
357 unidentified aliphatic compounds was also present in this material. The more
358 concentrated phenolic or olefinic compounds were largely successfully separated by
359 HPLC and identified for 2D NMR, providing a representative cross section of the
360 types of compounds present in the leachate. These included three flavonoids
361 (quercetin 3-glucoside, kaemferol 3-glucopyranoside and kaempferol 3-galactoside),
362 two tannins (ellagic acid and gallic acid), three phenolic glycosides (chromones)
363 (isobiflorin, 8- β -C-glucopyranosyl-5,7-dihydroxy-2-isobutylchromone and
364 noreugenin) and two carotenoids (megastigmene) derivatives (corchoionoside C and
365 corchoionol C). Other compounds identified included a glycoside (1-methylethyl β -D-
366 glucopyranoside) and two glycosylated monoterpenes (6,7-dihydroxy-
367 dihydrolinalool-3-O- β -D-glucopyranoside and betulalbuside A) partial structures for
368 other coeluting and/or minor components from the HPLC column were identified,
369 established from ¹H and 2D NMR analysis, which were consistent with mono- and

370 sesquiterpenes. This suggests that the terpenes were the most numerous class of
371 compounds present in the sample. The presence of these additional terpenes was not
372 unexpected as over 60 mono- or sesquiterpenes have previously been characterized
373 from *E. tereticornis* (Singh et al., 2009)

374 During the mesocosm experiment, there were no statistical differences in SUVA
375 (proxy for DOC aromaticity) measures between treatments, while a_{350} (lignin
376 phenol content) and a_{440} (gilvin content) were statistically higher in the 25 mg L⁻¹
377 DOC treatment on Day 0 (also higher on Day 10 but not enough replicates for
378 analysis) (Table 3). SR (negatively correlated with DOM molecular weight) was
379 statistically lower in the 25 mg L⁻¹ DOC treatment compared to the 2 and 3.3 mg L⁻¹
380 DOC treatments on Day 0, but there were no differences in SR between treatments
381 on Days 3 or 10.

382 3.1.2 Physicochemical parameters

383 Values for some physicochemical parameters differed statistically between
384 treatments with greater differences typically earlier in the experiment just after
385 *Eucalyptus* leachate addition. Over the experiment, the 5.9 and 25 mg L⁻¹ DOC
386 treatments had statistically lower mean dissolved oxygen (DO) (2.46 and 5.06 mg L⁻¹
387 respectively) than the other treatments, and the ambient water (range 6.99 – 8.10
388 mg L⁻¹) (Table 2). Logging of DO every 15 min in the control, 2 and 25 mg L⁻¹ DOC
389 treatments (one mesocosm each) showed similar daytime DO concentrations in the
390 control and 2 mg L⁻¹ DOC treatments, but a greater night-time sag in DO
391 concentrations in the 2 mg L⁻¹ DOC treatment, compared with the control (Fig. 1). In
392 comparison, in the 25 mg L⁻¹ DOC treatment, there was a rapid reduction in DO
393 concentrations over the first two days, then values remained close to zero until
394 logging stopped on day 5.

395 pH was statistically lower in the 3.3, 5.9 and 25 mg L⁻¹ DOC treatments across the
396 experiment (values 8.0 – 9.2) compared with ambient water and the other
397 treatments (values 9.5 – 9.7) (Table 2). Secchi depth was statistically lower in the 2.0
398 and 25 mg L⁻¹ DOC treatments (0.55 – 0.74 m) compared with the other treatments.
399 The calculated euphotic depth for the ambient water was 4.4 m, based on PAR
400 measurements. This compared with a bag depth of ~ 3 m. In the case of temperature,
401 there were no statistical differences between treatments. Specific conductivity across
402 treatments ranged from a mean of 0.603 to 0.620 mS cm⁻¹, with the 5.9 and

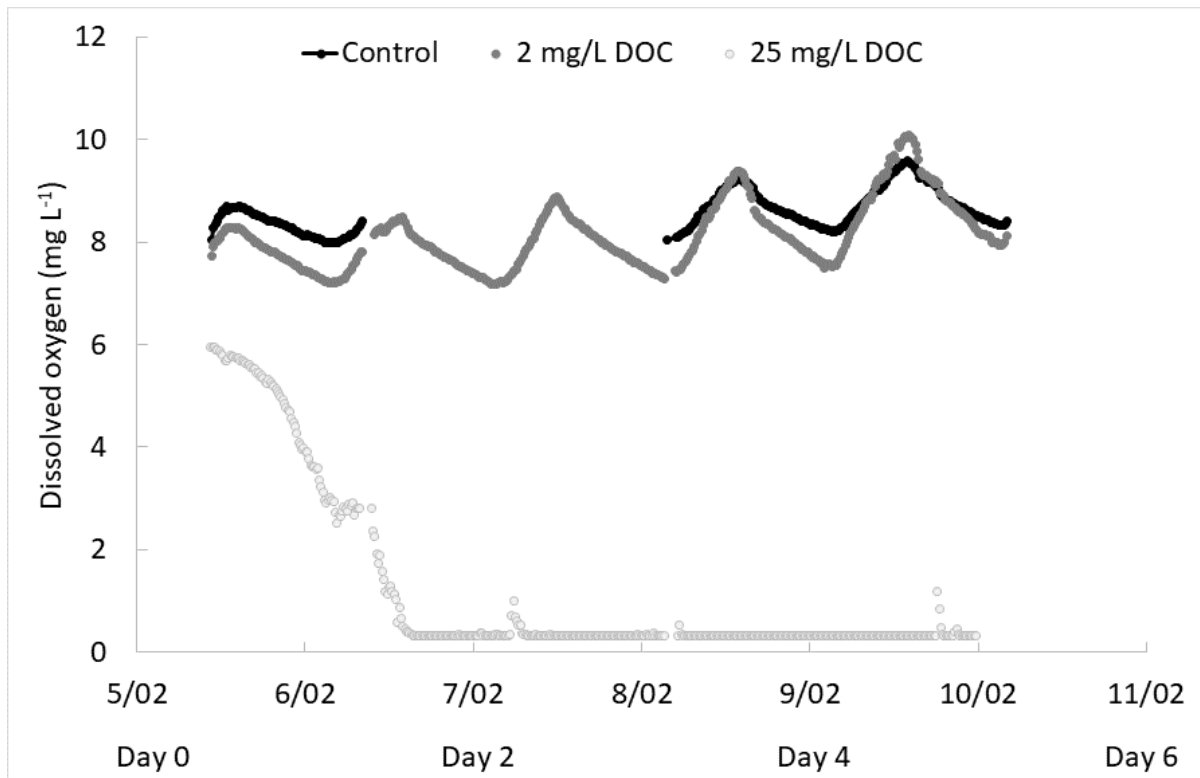
403 25 mg L⁻¹ DOC treatments having significantly higher specific conductivities (Table
 404 2). Turbidity ranged from 6.0 to 11.2 NTU, and was statistically highest in the
 405 2 mg L⁻¹ DOC treatment.

406

407 *Table 2: Mean (SD) of physicochemical parameters measured across the entire*
 408 *experiment in each treatment. Significant differences (P<0.05) between treatments*
 409 *shown as a, b, c, d. DO = dissolved oxygen, Sp. Cond. = specific conductivity.*

DOC conc (mg L ⁻¹)	Temperature (°C)	DO (mg L ⁻¹)	pH	Sp. Cond. mS cm ⁻¹	Turbidity (NTU)	Secchi depth (m)
Ambient	27.76 (0.63) ^a	7.56 (0.85) ^{ab}	9.7 (0.2) ^a	0.603 (0.004) ^{ab}	7.4 (0.3) ^{abc}	1.03 (0.15) ^a
0	27.49 (0.36) ^a	8.10 (0.34) ^a	9.7 (0.1) ^a	0.600 (0.003) ^a	9.3 (1.8) ^{ad}	0.84 (0.10) ^{ab}
2	27.45 (0.41) ^a	7.94 (0.52) ^a	9.6 (0.1) ^a	0.602 (0.003) ^a	11.2 (3.0) ^d	0.74 (0.07) ^c
3.3	27.54 (0.37) ^a	6.99 (0.50) ^b	9.2 (0.2) ^b	0.607 (0.005) ^{bc}	8.1 (3.1) ^b	0.81 (0.12) ^{bc}
5.9	27.57 (0.38) ^a	5.04 (1.37) ^c	8.5 (0.4) ^c	0.612 (0.004) ^c	5.5 (2.5) ^c	0.85 (0.23) ^{abc}
25	27.58 (0.39) ^a	2.46 (1.79) ^d	8 (0.3) ^d	0.620 (0.005) ^d	6.0 (1.4) ^c	0.55 (0.13) ^d

410



411

412 *Figure 1: Dissolved oxygen concentrations (mg L⁻¹) logged every 15 min in three*
 413 *mesocosms (control, 2 and 25 mg L⁻¹ DOC addition) treatments over the course of*
 414 *the experiment.*

415

416 3.1.3 Nutrient and chlorophyll *a* parameters

417 DON, DOP and DOC concentrations were statistically higher in 5.9 and 25 mg L⁻¹
 418 DOC treatments over the whole experiment compared with the control, 2 and 3.3 mg
 419 L⁻¹ DOC treatments (Table 3, Fig. 2). Concentrations in the 5.9 and 25 mg L⁻¹ DOC
 420 treatments decreased in the first three days of the experiment. In the 25 mg L⁻¹ DOC
 421 treatments there was a 40, 20 and 25% decrease in DOC, DON and DOP
 422 concentrations respectively. The rate of decrease was less between days 3 and 10. The
 423 background DOC concentration in the adjacent ambient reservoir water was 6.85 ±
 424 1.09 mg L⁻¹.

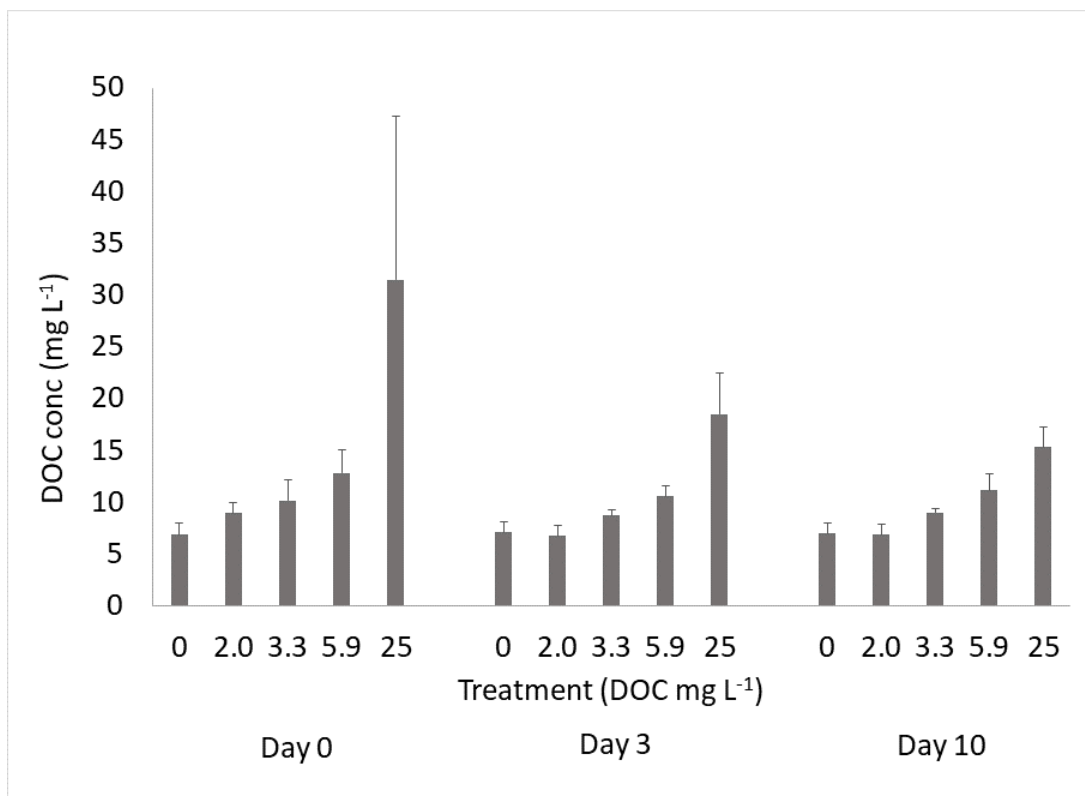
425 Ammonium concentrations were higher overall in the 5.9 and 25 mg L⁻¹ DOC
 426 treatments compared with the control and 2 mg L⁻¹ DOC treatments (Table 3, Fig. 3).
 427 Differences were greatest on day 0, with the 25 mg L⁻¹ DOC treatment having 0.093 ±
 428 0.033 mg N L⁻¹ compared with 0.010 ± 0.001 mg N L⁻¹ in the control. After this time,
 429 ammonium concentrations decreased (as measured on days 3 and 10). Nitrate

430 concentrations were close to the detection limit in all treatments across the
431 experiment (Table 3). Phosphate concentrations were statistically higher in the 5.9
432 and 25 mg L⁻¹ DOC treatments than the control and 2 mg L⁻¹ DOC treatment (Table 3,
433 Fig. 2). However, concentrations did not decrease over the experiment.

434 There were no statistical differences in TN concentrations between treatments, while
435 TP concentrations were higher in the 3.3, 5.9 and 25 mg L⁻¹ treatments compared
436 with the control (Table 3). The log-transformed molar TN:TP ratios were high to very
437 high in all treatments, compared with Redfield ratios (Redfield, 1958, Isles 2020)
438 except the 25 mg L⁻¹ DOC treatment. Molar PN:PP were also relatively high in the
439 control and 2 mg L⁻¹ DOC treatments.

440

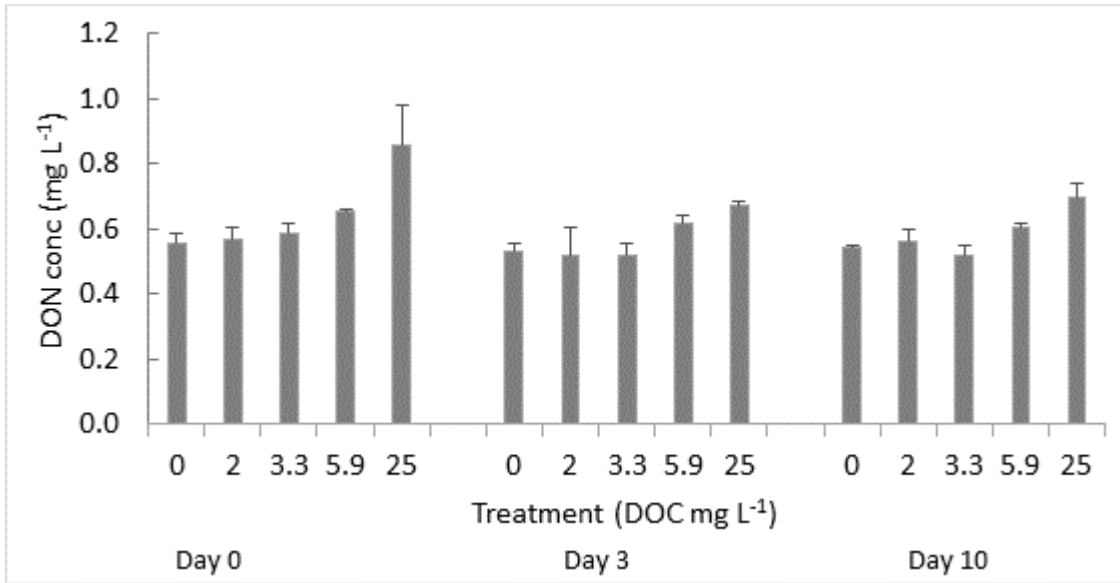
441 (a)



442

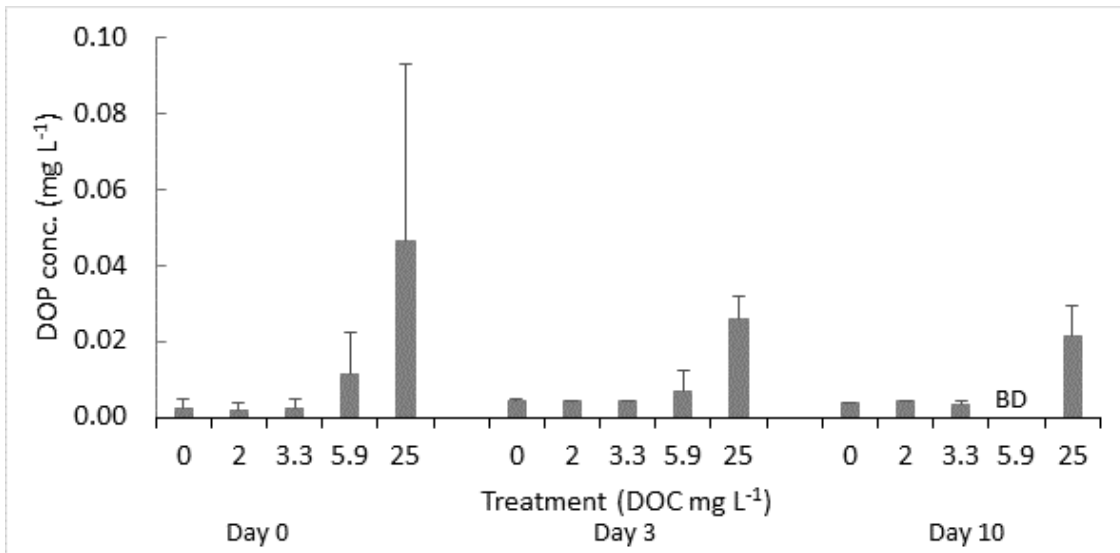
443

444 (b)



445

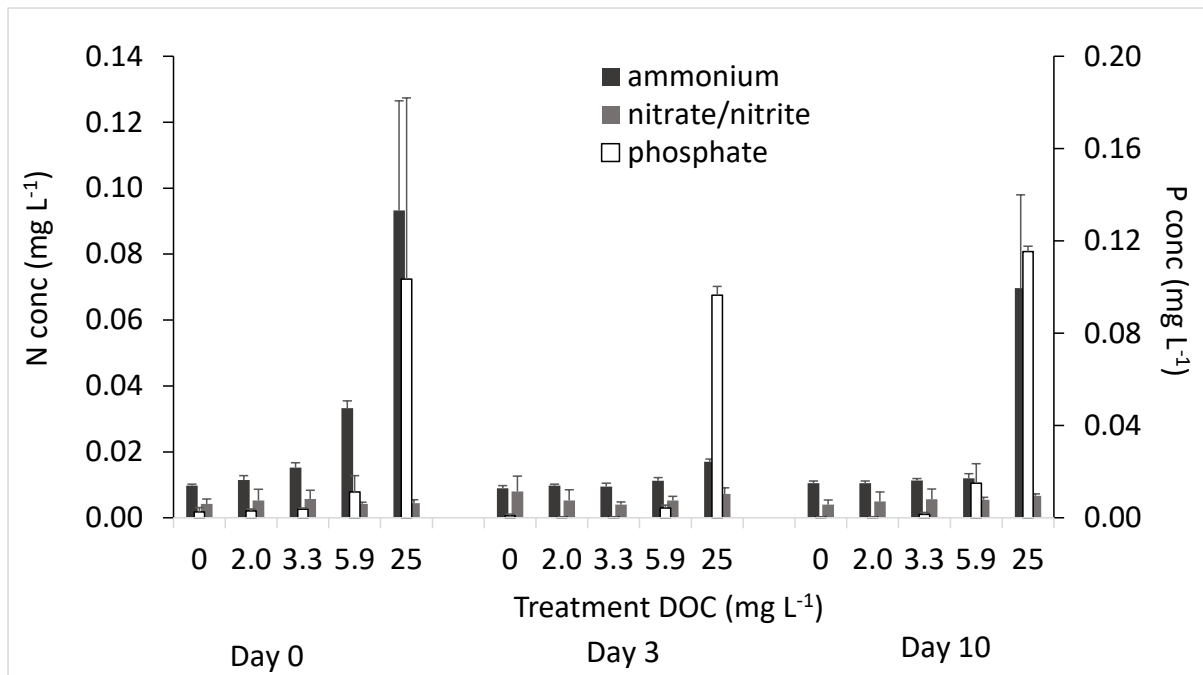
446 (c)



447

448 *Figure 2: Mean (SD) of (a) DOC, (b) DON, and (c) DOP concentrations (mg L⁻¹)*
 449 *measured in each treatment on days 0, 3 and 10 of the experiment. BD = below*
 450 *detection limit.*

451

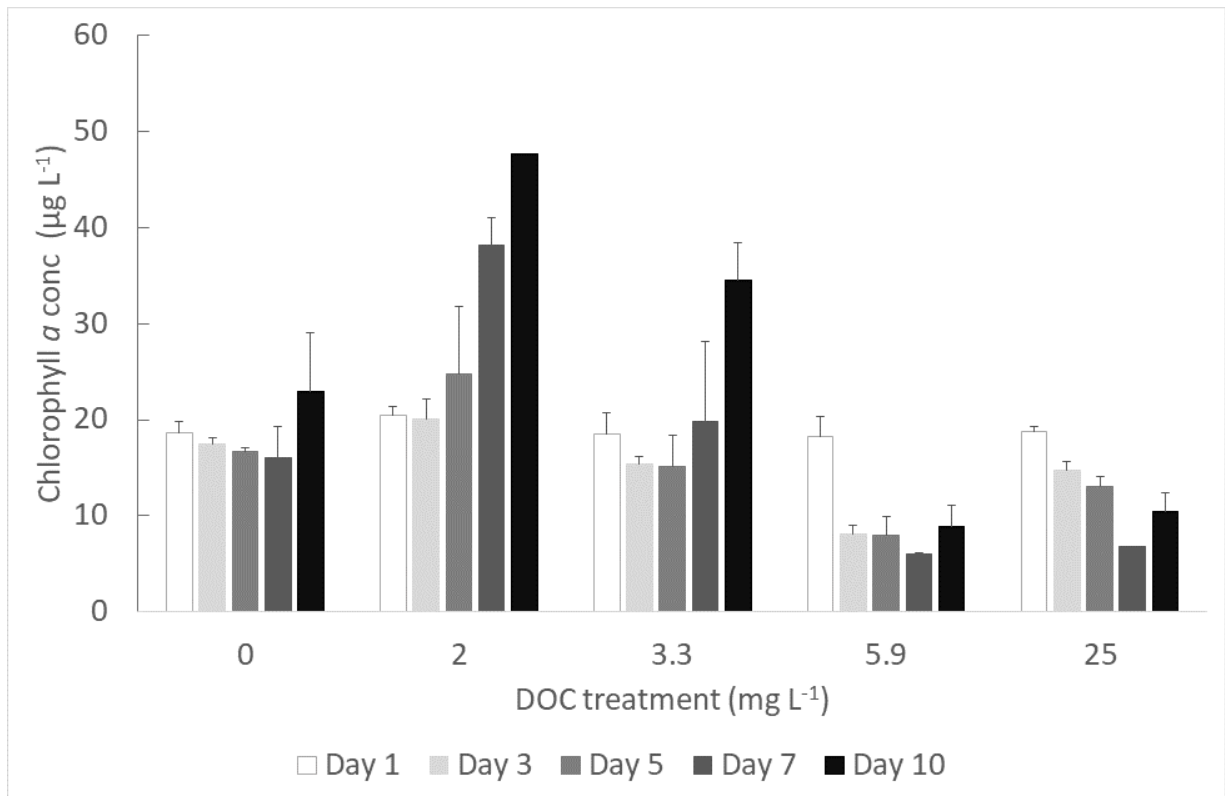


452

453 *Figure 3: Mean (SD) of ammonium, nitrate/nitrite and phosphate concentrations*
 454 *(mg L⁻¹) in each treatment on days 0, 3 and 10 of the experiment.*

455

456 Over the whole experiment, chlorophyll *a* concentrations were statistically lower in
 457 the 5.9 and 25 mg L⁻¹ treatments compared with the 2 and 3.3 mg L⁻¹ treatments
 458 (Table 3). This effect is clearly seen on day 3 and was sustained throughout the
 459 remainder of the experiment (Fig. 4). Chlorophyll *a* concentrations in the 2 mg L⁻¹
 460 DOC addition increased more rapidly than in the control.



461

462

463 *Figure 4: Mean (SD) of chlorophyll a concentrations ($\mu\text{g L}^{-1}$) in each treatment on*
 464 *days 1, 3, 5, 7 and 10 of the experiment.*

Table 3: Mean (SD) of nutrient, organic carbon, and other parameters in each treatment across the entire experiment. Significant differences between treatments shown as a, b, c, d. Chl a = chlorophyll a, A440 = Gilvin content, SR = ratio of slopes.

Treat ment: DOC (mg L ⁻¹)	Ammonium	Nitrate	Phosphate	Total N	Total P	DON	DOP	DOC	Log mol TN:TP	Log mol PN:PP	Chl a	a440	SR
	Conc mg L ⁻¹										Conc µg L ⁻¹		
AMB	0.010 (0.001) ^a	0.005 (0.001)	0.001 (0.001) ^a	0.76 (0.08) ^a	0.01 (0.01) ^a	0.512 (0.022) ^a	0.004 (0.001) ^{ab}	7.35 (0.86) ^a	2.2		19.15 (0.94) ^a	2.99 (6.05) ^a	0.72 (0.13) ^a
0	0.010 (0.001) ^a	0.006 (0.003)	0.002 (0.001) ^a	0.83 (0.17) ^{ab}	0.01 (0.01) ^a	0.545 (0.027) ^a	0.003 (0.001) ^a	7.02 (0.95) ^a	2.4	2.7	25.85 (16.72) ^{ab}	5.02 (8.10) ^{ab}	0.71 (0.14) ^a
2	0.011 (0.001) ^a	0.005 (0.003)	0.001 (0.001) ^a	0.94 (0.18) ^{ab}	0.03 (0.01) ^{ab}	0.542 (0.061) ^a	0.004 (0.001) ^a	7.67 (1.44) ^a	1.9	1.7	33.29 (9.79) ^a	3.92 (6.46) ^{ab}	0.86 (0.16) ^b
3.3	0.012 (0.003) ^{ab}	0.005 (0.002)	0.004 (0.006) ^{ab}	0.84 (0.11) ^{ab}	0.05 (0.01) ^{bc}	0.559 (0.049) ^a	0.003 (0.002) ^a	9.35 (1.31) ^a	1.6	1.3	26.73 (17.13) ^a	2.83 (1.36) ^{ab}	0.87 (0.08) ^b
5.9	0.033 (0.027) ^b	0.005 (0.001)	0.029 (0.045) ^{bc}	0.91 (0.17) ^{ab}	0.11 (0.05) ^c	0.652 (0.044) ^b	0.013 (0.009) ^{bc}	11.61 (1.86) ^b	1.4	0.8	8.69 (4.51) ^c	5.39 (3.06) ^{bc}	0.81 (0.06) ^{ab}
25	0.048 (0.043) ^b	0.006 (0.002)	0.084 (0.060) ^b	1.08 (0.21) ^b	0.20 (0.12) ^c	0.712 (0.146) ^b	0.028 (0.019) ^c	22.39 (11.59) ^c	1.0	0.9	12.22 (5.97) ^{bc}	12.88 (7.33) ^c	0.71 (0.08) ^a

466

467 3.1.4 Phytoplankton and bacterial data

468 The cyanobacterial species, *R. raciborskii* was the dominant species in the
469 phytoplankton community for the duration of the experiment, based on cell counts
470 (49% on day 0). At the start of the experiment, *R. raciborskii* cell densities in the
471 ambient water were $162,000 \pm 31,000$ cells mL⁻¹. In the control, *R. raciborskii*
472 densities increased to 241,000 cells mL⁻¹ by day 10 (Table S2, Fig. 5a). On day 5,
473 *R. raciborskii* cell densities were statistically lower in the 5.9 and 25 mg L⁻¹
474 treatments compared with the other treatments. By day 10, densities in the 25 mg L⁻¹
475 treatment were relatively low, but highly variable between replicates, i.e. $68,283 \pm$
476 $129,376$ cells mL⁻¹, while densities in the other treatments ranged from 230,000 to
477 380,667 cells mL⁻¹.

478 The cyanobacterial filamentous genus, *Planktolylnbya* spp. and the
479 picocyanobacterial genus, *Cyanogranis* spp. were also subdominant species (25 and
480 14% on day 0). The species composition and species dominance were very similar in
481 the adjacent ambient water on days 0 and 10 of the experiment (Table S3). At the
482 start of the experiments, total cyanobacterial densities were $330,000 \pm 41,000$ cells
483 mL⁻¹. Densities were lower overall in the 5.9 and 25 mg L⁻¹ DOC treatments
484 compared with the other treatments (Fig. 5b). Chlorophyte cell densities were very
485 low, by comparison to cyanobacterial densities (typically <10,000 cells mL⁻¹), and
486 there were no statistical differences between treatments. Bacillariophyte cell
487 densities were also low (typically <10,000 cells mL⁻¹), and lower in the 5.9 and 25 mg
488 L⁻¹ DOC treatments compared with the other treatments (Table S2). There were no
489 statistical differences between the bacterial densities on day 3, except for the 25 mg
490 L⁻¹ DOC treatment which had higher densities, i.e. $12,992,500 \pm 5,282,950$ cells mL⁻¹
491 compared with $3,245,000 \pm 522,143$ cells mL⁻¹ in the control (Table S2). Rod shaped
492 bacteria increased in densities more rapidly than either filamentous or spherical
493 cells.

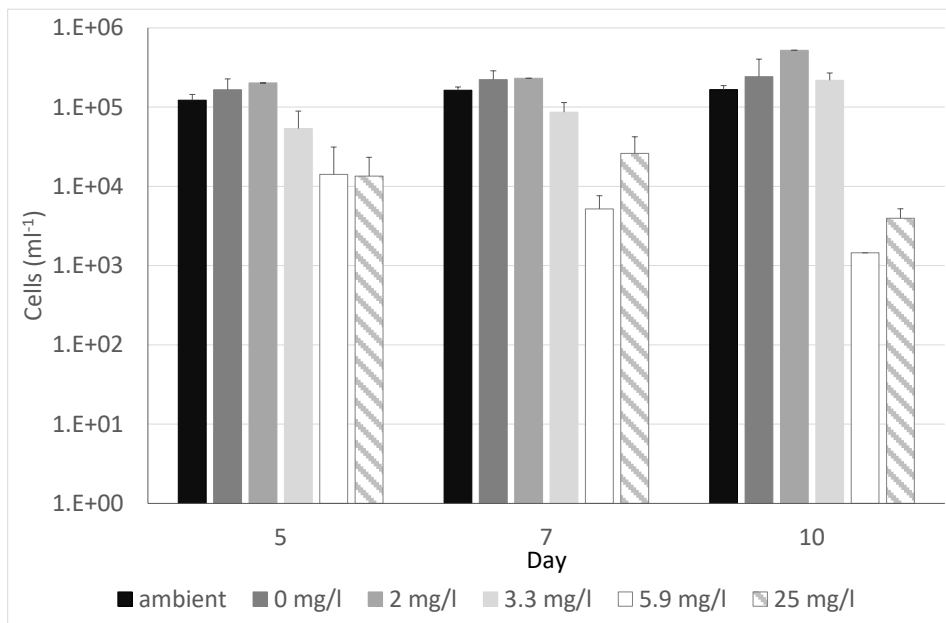
494 Photosynthetic yields (Fv/Fm) of the cyanobacteria (blue group), as measured using
495 a PHYTOPAM (Walz), were statistically lower in the 5.9 and 25 mg L⁻¹ DOC
496 treatments compared with the control and 2 mg L⁻¹ DOC treatment on days 0 and 1
497 (Table 4). From day 3 onwards, there were no statistical differences between
498 treatments and the control (Fig. 6). In contrast the yield (Fv/Fm) values of the brown

499 group, primarily bacillariophytes, showed no statistical differences between
500 treatments. The yield (Fv/Fm) values for the green group, i.e. chlorophytes, was too
501 low for meaningful measurements.

502

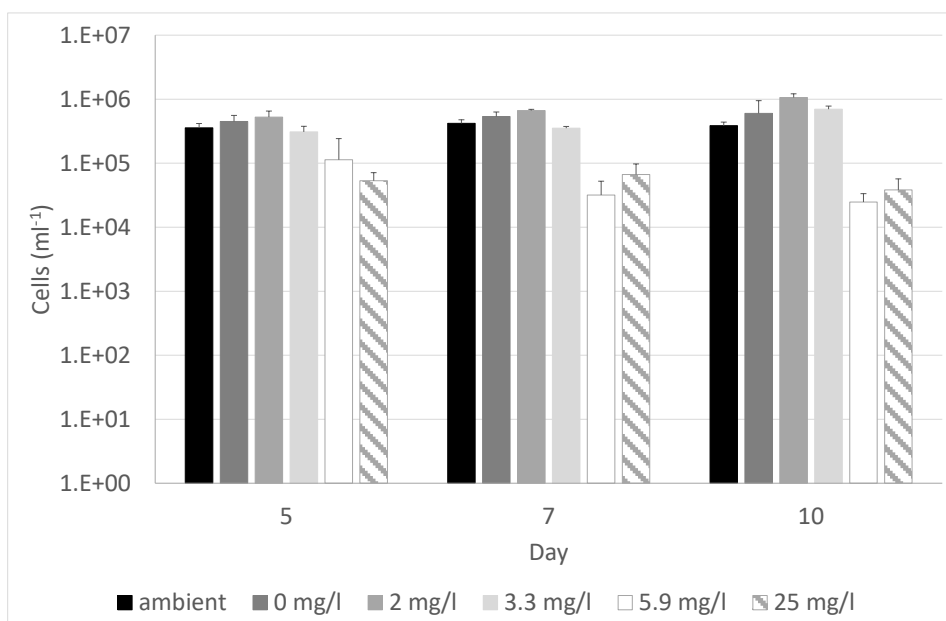
503 *Figure 5: (a) Raphidiopsis raciborskii and (b) total cyanobacterial cell densities*
504 *(cells mL⁻¹) for each treatment on days 5, 7 and 10 of the experiment. Note: log*
505 *scale.*

506 (a)



507

508 (b)



509

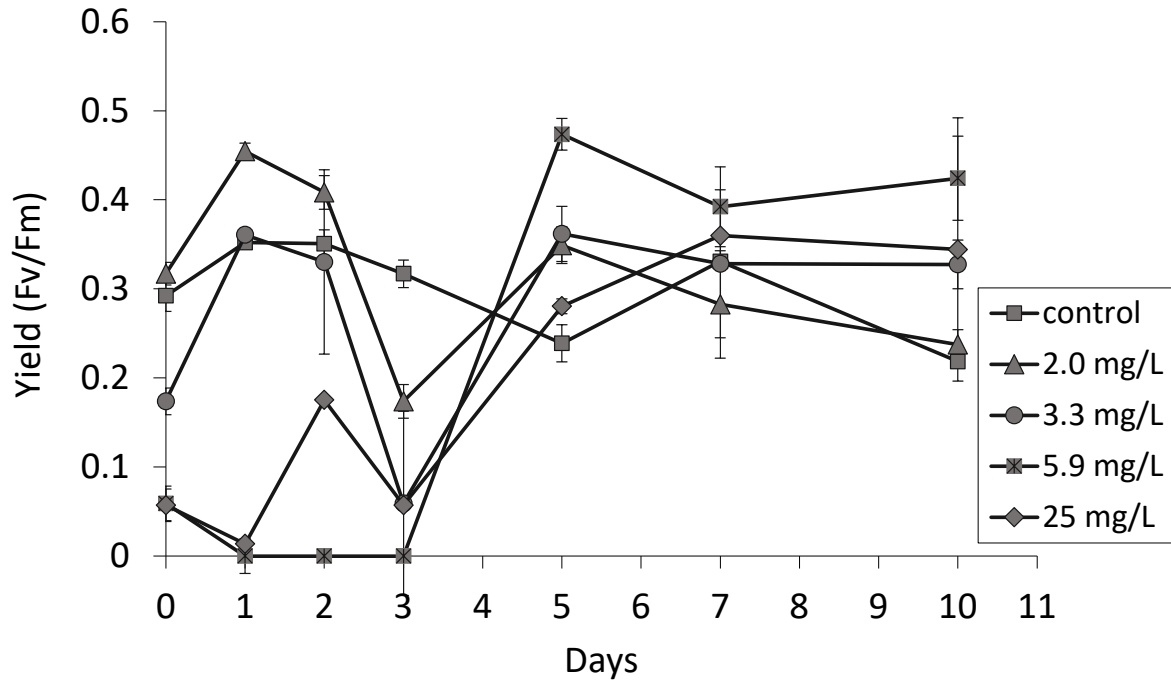


Figure 6: Mean (SD) of photosynthetic yield (F_v/F_m) for all treatments across the experiment.

Table 4: Mean (SD) of photosynthetic yield (F_v/F_m) of the blue channel, i.e. cyanobacteria, for all treatments across the experiment. Significant differences shown as a, b, c, d showing differences between treatments in individual days.

Treatment DOC (mg L ⁻¹)	Day 0	Day 1	Day 2	Day 3	Day 5	Day 7	Day 10
AMB	0.31 (0.02) ^a	0.38 (0.02) ^{ab}	0.37 (0.01) ^{ab}	0.30 (0.00)	0.19 (0.03) ^a	0.26 (0.02)	0.33 (0.03)
0	0.29 (0.04) ^a	0.35 (0.06) ^{ab}	0.35 (0.03) ^{ab}	0.21 (0.15)	0.24 (0.04) ^{ab}	0.33 (0.13)	0.22 (0.03)
2	0.32 (0.03) ^a	0.45 (0.01) ^a	0.41 (0.04) ^a	0.28 (0.19)	0.35 (0.04) ^{bc}	0.28 (0.13)	0.24 (0.03)
3.3	0.17 (0.03) ^{ab}	0.36 (0.02) ^{ab}	0.33 (0.22) ^{ab}	0.22 (0.17)	0.36 (0.07) ^{bc}	0.33 (0.18)	0.33 (0.05)
5.9	0.06 (0.04) ^b	0.00 (0.00) ^b	0.00 (0.00) ^c	0.00 (0.00)	0.47 (0.04) ^b	0.39 (0.10)	0.42 (0.05)
25	0.06 (0.04) ^b	0.01 (0.03) ^b	0.18 (0.01) ^{bc}	0.19 (0.02)	0.28 (0.02) ^{ab}	0.36 (0.06)	0.34 (0.29)

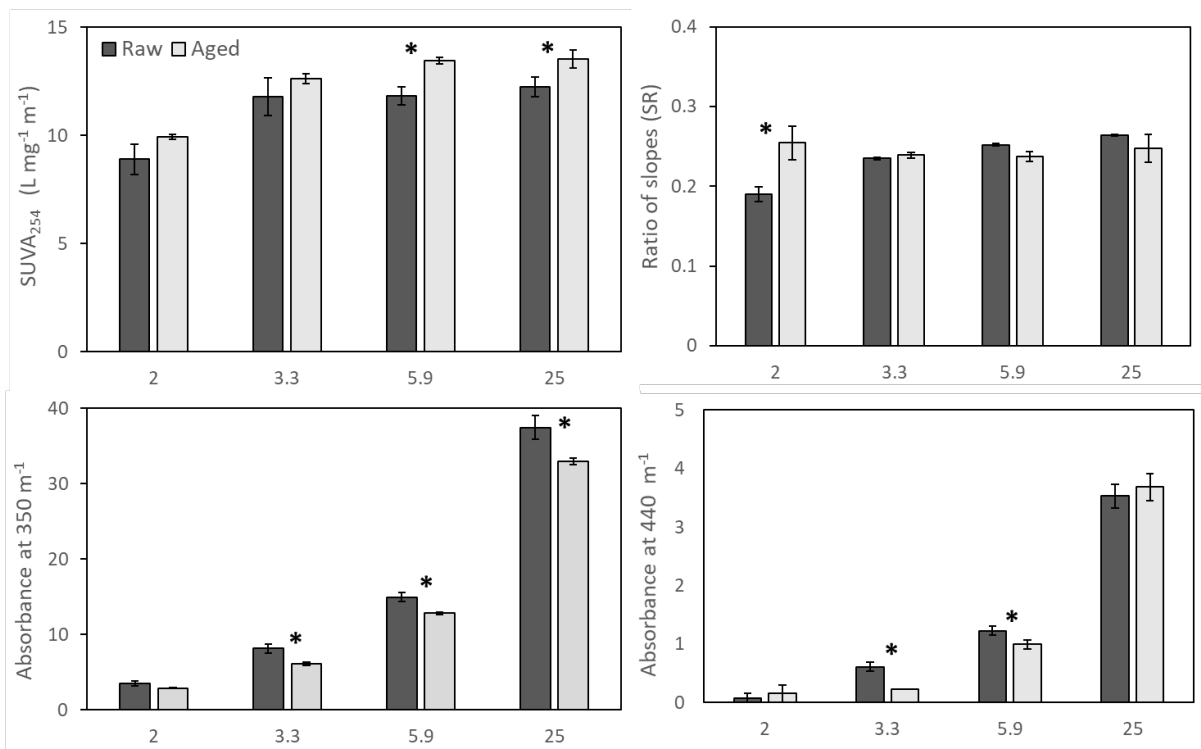
508 3.2 tDOM incubation experiment

509 An additional experiment was conducted to determine the effect of sunlight on tDOM
510 measures in the *Eucalyptus* leachate, diluted with DI water to the same
511 concentration (25 mg L⁻¹ DOC) as those used in the mesocosm treatments. This
512 experiment was conducted in the absence of lake water. SUVA/DOM aromaticity,
513 a₃₅₀ (proxy for lignin phenol) and a₄₄₀ (proxy for gilvin/water colour) increased
514 with increasing tDOM addition both before and after 5 days of aging (Fig. 7). Aging
515 significantly increased SUVA in the 5.9 and 25 mg L⁻¹ DOC treatment, whereas aging
516 reduced lignin-phenol and gilvin content in most treatments. There were few
517 differences in SR between treatments or following aging.

518 Comparison of the ¹H-NMR spectra before and after 5 d of aging for the 25 mg L⁻¹
519 DOC treatment only, indicates there have been changes in the complexity and
520 abundance of the oxygenated aromatic compounds present (6-8 ppm region, Fig.
521 S4). 2D-NMR techniques (HSQC and HMBC) confirmed the presence of multiple
522 sugars, myo-inositol (microbial metabolite of glucose), as well as fatty acids in all
523 samples (Figs. 8, S5). Carboxylic acids, formic and acetic and hydroxypropanoic acid
524 were also present, as were range of aromatic compounds, including gallic acid.
525 Amino acids, sugars and their derivatives were present in greater relative
526 proportions than the aromatic compounds.

527 The relative proportions of all detected compounds decreased significantly following
528 5 days of aging. The relative proportion of fatty acids, sugars and gallic decreased by
529 around 60%, whereas the relative proportion of flavonoids and myo-inositol
530 decreased by 45 and 35% respectively (Fig. 8). The intensity of peaks associated
531 amino acids also decreased following aging, but signals were also associated with
532 other compound classes and therefore were not quantified.

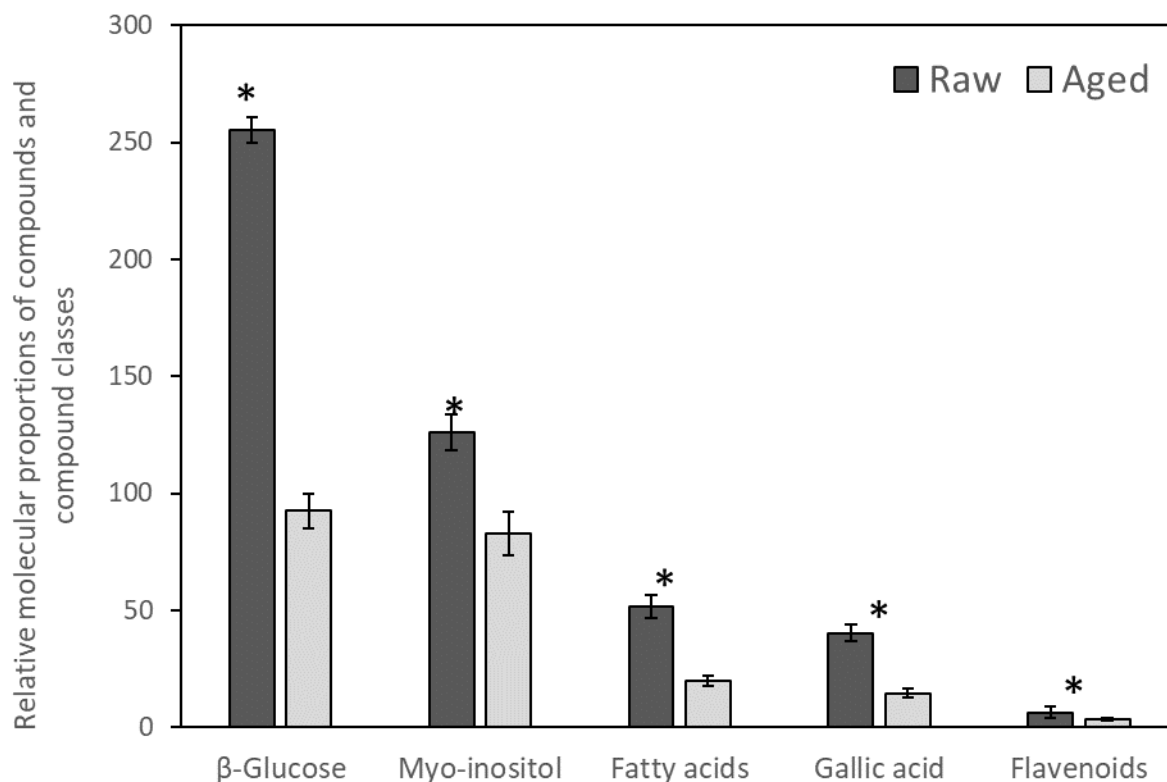
533



534

535 *Figure 7: tDOM composition as described by absorbance metrics in tDOM*
 536 *incubation experiment for raw samples and those aged in sunlight for 5 days. Data*
 537 *are mean ± standard error for: specific UV absorbance at 254 nm (SUVA₂₅₄; L*
 538 *mg⁻¹ m⁻¹); the ratio of slopes (SR), a metric negatively correlated with DOM*
 539 *molecular weight; and absorbance at 350 nm (a₃₅₀) and 440 nm (a₄₄₀) which are*
 540 *proxies for lignin phenol and gilvin concentrations respectively. * denotes*
 541 *significant (P < 0.05) differences between raw and aged treatments for each tDOM*
 542 *measure.*

543



544

545 *Figure 8: Mean (SD) of tDOM composition (relative molecular proportions of*
 546 *compounds and compound classes quantified using NMR spectroscopy) of samples*
 547 *diluted to 25 mg L⁻¹ DOC in the tDOM incubation experiment on day 0 (raw) and*
 548 *after exposure to sunlight for 5 days. * denotes significant (P<0.05) differences*
 549 *between raw and aged treatments for each group of compounds.*

550

551 **4. Discussion**

552 This mesocosm study showed that tDOM from *Eucalyptus* leaf leachate added to a
 553 lake with moderate DOC concentrations, i.e. ~ 7 mg L⁻¹, and a naturally occurring
 554 cyanobacterial bloom dominated by the toxic species, *Raphidiopsis raciborskii*,
 555 negatively impacted photosynthesis and cell densities., The impact was greatest in
 556 the highest DOC treatment, 25 mg L⁻¹ DOC. Other cyanobacteria were equally
 557 affected. Diatoms and chlorophytes were at relatively low densities throughout the
 558 experiment, but diatom densities were also impacted negatively by tDOM addition.

559 A previous laboratory culture study showed that photosynthesis of the cyanobacterial
 560 species, *R. raciborski* can be inhibited by exposure to leaf leachates of many
 561 terrestrial plant species (Neilen et al., 2017). The threshold DOC concentration for
 562 yield (Fv/Fm) inhibition of *R. raciborskii* by *Eucalyptus* leaves (the same species

563 used in our study) was higher than that for the current study (>20 mg L⁻¹ DOC for
564 fresh leachate) (Neilen et al., 2019). However, the background DOC concentration in
565 the reservoir in our study was ~ 7 mg L⁻¹ whilst the Neilen et al (2019) study had no
566 background DOC. Therefore, the differences between these two studies may not be
567 substantial.

568 Other studies have found that tDOM inputs can negatively affect algae. For example,
569 Deininger et al. (2017) also found that phytoplankton biomass and production
570 decreased using DOC concentrations similar to those in our study (ranging from 6.9
571 – 21 mg L⁻¹ DOC). However, in their experiment, the phytoplankton community
572 composition changed from a predominance of non-flagellated species to flagellated
573 species dominance as lake DOC concentrations increased. A study of lake browning
574 showed that clear oligotrophic lakes tended to be dominated by diatoms, while low
575 levels of browning (4-8 mg L⁻¹ DOC) promoted cyanobacteria, and higher
576 concentrations of DOC, i.e. 8-12 mg L⁻¹, promoted mixotrophic species (Senar et al.,
577 2021). Urrutia-Cordero et al., (2017) also showed that phytoplankton biodiversity
578 decreased with brownification and warming, with an increase in mixotrophic species
579 and reduction in diatoms and chlorophytes. In our study, cyanobacteria dominated
580 with a DOC concentration in the reservoir of ~7 mg L⁻¹. However, this was not a lake
581 with coloured DOC. Therefore, the dominance of cyanobacteria at a particular DOC
582 concentration in our study is unlikely to be directly comparable with studies in
583 coloured lakes.

584 There are a number of potential explanations for the inhibitory effect of tDOM on
585 phytoplankton cell densities and photosynthesis including: phytotoxic effects;
586 reduced light availability from coloured water; and a reduction in water temperature
587 due to shading effects. A previous laboratory study using the same *Eucalyptus*
588 species as our study examined which compounds inhibited the photosynthetic yield
589 (Fv/Fm) of *R. raciborskii*. The study found that the phytotoxic compounds were
590 gallic acid and polyphenols (Neilen et al., 2020). Gallic acid and ellagic acid were
591 identified in the *Eucalyptus* leachate in the present study, as well as polyphenolic
592 compounds such as flavonoids and phenolic glycosides. It would be expected that
593 those compounds would also impact *R. raciborskii* in the current experiment,
594 especially early in the study. Many terpenes were also present in the *Eucalyptus*
595 leachate, based on NMR analysis. A previous study found terpenes associated with

596 degradation of birch, spruce and pine (Kanerva et al., 2008) and a range of bacterial-
597 derived terpenes with algacidal properties have been identified (Meyer et al., 2017).
598 It is possible that terpenes may have impacted the phytoplankton community in our
599 study. Chemical interactions associated with tDOM may also inhibit cyanobacteria,
600 e.g. Nagai et al., (2006) showed that DOM complexed with iron, causing iron
601 limitation, inhibiting phytoplankton growth.

602 Other studies have suggested that the negative effect of tDOM on phytoplankton
603 growth may be due to reduced light availability, especially when the coloured
604 component is high. In our experiment, the 5.9 and 25 mg L⁻¹ DOC addition
605 treatments had lower Secchi readings than the control in the first 2 days, but after
606 this time there was no difference in the readings. *R. raciborskii* is known to be well
607 adapted to relatively low light levels, compared with many other phytoplankton
608 species (O'Brien et al., 2009; Xiao et al., 2017). Therefore, reduced light levels are
609 unlikely to be the dominant factor suppressing the cell densities of this species. Other
610 studies have found limited evidence of coloured tDOM affecting phytoplankton
611 growth. Lebret et al., (2018) showed that addition of humic substances to lakes,
612 which decreased light availability, did not change phytoplankton biomass or growth,
613 but changed species composition. Ekvall et al., (2013) also showed that the addition
614 of humics (from brown lakes) to mesocosms did not change the growth of the
615 cyanobacterial community. In a review of dissolved humic substances and their
616 ecological effect, Steinberg et al., (2006) identified that the reddish light of humic-
617 rich lakes can also differentially affect cyanobacteria as they appear to be unable to
618 use their accessory pigments (particularly phycocyanin) to exploit the this
619 wavelength of light . Additionally, there is evidence that increased coloured tDOM in
620 lakes may increase temperatures and thermal stratification in surface waters
621 (Caplanne and Laurion, 2008; Pilla et al., 2018). However, surface water
622 temperatures, ranging from around 27 to 28°C in our experiment, were the same
623 across treatments.

624 Counteracting the negative effects on phytoplankton, tDOM can also increase
625 nutrient inputs to waterways. Other studies have demonstrated a trade-off between
626 nutrients in coloured tDOM stimulating phytoplankton growth at lower
627 concentrations, and increasing light attenuation inhibiting phytoplankton growth at
628 higher tDOM concentrations (Seekell et al., 2015; Deininger et al., 2017; Isles et al.,

629 2021; Caldero-Pascual et al., 2021). In our study, ammonium and phosphate
630 concentrations were higher in the treatments with higher tDOM addition, providing
631 an additional nutrient source for phytoplankton. Phosphate concentrations in the
632 control and ambient water were very low, i.e. around or below detection limits
633 (0.002 mg P L⁻¹), and molar TN:TP ratios were high, relative to Redfield (1958).
634 Therefore, the addition of phosphate had the potential to promote growth and may
635 be reflected in the short-term increase in photosynthetic yield (Fv/Fm) in the 2 mg L⁻¹
636 DOC treatment. However, once DOC concentrations were above 3.3 mg L⁻¹, it was
637 clear that negative effects of tDOM outweighed any potential positive effects of
638 phosphate (and ammonium) addition on phytoplankton. Indeed, phosphate
639 concentrations in the treatments with higher tDOM concentrations did not decrease
640 over the study, indicative of a lack of utilization of phosphate by the phytoplankton
641 community. *R. raciborskii* has been shown to be very efficient at rapid phosphate
642 uptake and storage to excess when growing (Willis et al., 2017; Xiao et al., 2020).
643 Some fractions of DON and DOP pools are also available for growth of
644 phytoplankton, e.g. urea, free amino acids, glucose 6-phosphate (Mackay et al.,
645 2020). However, given the relatively high concentrations of more bioavailable forms
646 of nitrogen and phosphorus, i.e. ammonium and phosphate, in the treatments, these
647 are likely to be the primary nutrient sources, rather than DON and DOP.

648 One of the challenges of studies of tDOM in the field is that terrestrial sources of
649 DOM cannot be differentiated from autochthonous sources of DOM in terms of their
650 ecosystem effects. In our study there was a background DOM load, i.e. ~7 mg L⁻¹
651 DOC which was likely to be primarily autochthonous in nature, given the large size of
652 the reservoir, ongoing algal blooms, and lack of catchment inflows prior to the study.
653 The chemical characteristics of autochthonous DOM was likely to be very different to
654 that of the tDOM, and therefore understanding the source of transformations of
655 tDOM in the field is problematic. Therefore, our approach of combining a small-scale
656 study of tDOM transformations in the absence of autochthonous DOM, with the
657 mesocosm study of DOM transformations was an attempt at addressing this
658 challenge.

659 In our study, a range of tDOM compounds decreased by similar amounts over the
660 study, including fatty acids, sugars, and gallic acid. Flavonoids and myo-inositol also
661 decreased by a lesser amount. Gallic acid is known to inhibit photosynthesis in *R.*

662 *raciborskii* (Neilen et al., 2020) as well as *Microcystis*, although Laue et al., (2014)
663 found a more pronounced effect in the laboratory than in the field. In a small-scale
664 study, Neilen et al., (2019) showed that exposure to sunlight exacerbated the toxic
665 effect of tDOM leached from *Eucalyptus* leaves, despite no increase in the identified
666 toxic compounds. The production of reactive oxygen species (ROS) was proposed as
667 a possible mechanism for inhibition of photosynthesis. It is, therefore, possible that
668 ROS may also have played a role in the current study, but further work is needed to
669 understand the role of ROS, and more broadly, the physiological mechanisms for the
670 effect of tDOM on cyanobacteria (Steinberg et al., 2006).

671 Our study showed that microbial densities increased and DO levels decreased with
672 higher tDOM, and at the same time, there was a decrease in ammonium, DOC, DON
673 and DOP concentrations. The effect was greatest in the 25 mg L⁻¹ treatment. The
674 anoxic conditions in the 25 mg L⁻¹ DOC treatment which developed one day after
675 tDOM addition was likely to have affected biogeochemical processes, including
676 transformations of organic matter. However, the interplay between this and
677 photolysis in terms of impacting transformations is unclear. The microbial
678 community may also be utilize DOC/DON/DOP compounds and ammonium either
679 directly from tDOM, or indirectly from degrading phytoplankton cells impacted by
680 tDOM. A previous study of DOM in river water showed that biodegradation was
681 primarily responsible for DOC remineralization, and losses of the amino acid
682 component of DOM, whereas photodegradation was primarily responsible for losses
683 of the chromophoric and lignin phenol components of DOM (Benner and Kaiser,
684 2011). Another study showed that the ratios of bioavailable DOC:reactive nitrogen
685 (sum of bioavailable DON and DIN) and bioavailable DOC:reactive P exerted a
686 strong stoichiometric control on reactive nitrogen and phosphorus uptake, and
687 quantified the range of C:N:P ratios at which maximum reactive N uptake occurred
688 (Graeber et al., 2021). A study of the use of tDOM by the microbial community in a
689 lake and its inlet suggested that microbes grew more on tDOM compared with
690 autochthonous sources within the lake (Stadler et al., 2020). The promotion of
691 microbial growth, as a result of tDOM inputs, may also have impacts on the
692 phytoplankton community. For example, microbes may produce compounds
693 inhibiting the growth of phytoplankton, or conversely increase the bioavailability of
694 nutrients (Seymour et al., 2017).

695 The tDOM aging experiment showed that all groups of organic compounds in the
696 leachate decreased over the experiment which may be related to the impact of either
697 biogeochemical processes and/or photolysis. The leachates also contained significant
698 amounts of sugars (α - and β -glucose) which were likely to be rapidly utilized by the
699 microbial community in the reservoir, as evidenced by the products of degradation of
700 these sugars, i.e. myo-inositol, as well as 2,3-butanediol. The leachates also contained
701 significant amounts of glycosylated compounds which may be hydrolyzed slowly,
702 providing a longer-term reservoir of glucose for microbial growth. The glycosidic
703 flavonoids, carotenoid derivative and terpenes present in the leachate would
704 gradually breakdown to feed further microbial metabolism. Therefore, in considering
705 the fate of tDOM in aquatic systems, it is also important to understand the
706 interactions between phytoplankton, microbes and physical processes, such as
707 photolysis.

708 Cyanobacterial blooms can be a major issue for water resources in freshwater aquatic
709 systems (e.g. O'Neil et al., 2012). This includes the globally prevalent toxic
710 cyanobacterial species, *R. raciborskii* (Burford et al., 2016). There is evidence that
711 climate change is increasing cyanobacterial blooms globally due to factors such as
712 increased water temperature and stratification (O'Neil et al., 2012). However, at the
713 same time, brownification of lakes is occurring in some regions of the world, with the
714 suggestion that climate change is a driver (Solomon et al., 2015; Creed et al., 2018).
715 This may be a counteracting factor for growth of cyanobacteria. Prediction of the
716 impacts of climate change on cyanobacteria have typically not included the trade-offs
717 between positive effects of climate change on growth of cyanobacteria, e.g. increased
718 temperature, stratification, and potential negative effects, e.g. increased coloured
719 tDOM in inhibiting growth. Factors such as climate-change driven increases in
720 rainfall/runoff events could increase tDOM inputs to lake and reservoirs. Our study
721 points to the importance of including the prediction of changes in tDOM inputs to
722 waterways, with flow-on effect on cyanobacterial blooms. However, it should be
723 acknowledged that the current study only examined short term effects. In the longer
724 term, effects of tDOM on phytoplankton may change, e.g. cyanobacterial species may
725 adapt to increasing tDOM inputs, Additionally, revegetation of catchments, for
726 example, may result in an increased frequency of pulses of tDOM to a reservoir
727 during rainfall/runoff events. Therefore, our results suggest that a longer term study
728 is warranted.

729 Our study showed that tDOM leached from *Eucalyptus* was beneficial in reducing
730 toxic cyanobacterial blooms, however, there are issues associated with treating
731 coloured tDOM for drinking water. Chlorination is typically used to treat tDOM
732 which results in the generation of disinfection byproducts (DBPs) (Muellner et al.,
733 2007). Studies have shown that some forms of DBPs can have negative effects on
734 human health. Franklin et al., (2021) showed that chlorinated leaf leachate from the
735 *Eucalyptus* species used in our study produced trihalomethanes (THMs), haloacetic
736 acids (HAAs), and haloketones after chlorination. Additionally, in ecotoxicological
737 studies, the chlorinated leachate induced oxidative stress in liver cells and bacterial
738 toxicity. Franklin et al. (2021) compared the results with another leachate of another
739 terrestrial tree, *Casuarina*, finding that different plant species result in different
740 DBPs being produced, as well as different ecotoxicological responses. Therefore,
741 consideration should be given to plant species when re-foresting catchments. It is
742 important that these tradeoffs are considered in terms of costs and benefits in
743 controlling algal blooms using tDOM.

744 **5. Conclusions**

745 In summary, this study showed that tDOM from the terrestrial plant, *E. tereticornis*
746 can negatively affect photosynthesis and biomass accumulation of the toxic
747 cyanobacterium, *R. raciborskii*, and other phytoplankton more broadly. The effect
748 was concentration dependent. It is likely phytotoxic compounds were the
749 predominant cause, but light availability for growth may also have had some impact.
750 The suite of compounds in tDOM, included those capable of inhibiting growth of
751 *R. raciborskii*, as well as also compounds such as glucose, which were likely to
752 stimulate microbial growth, and enhance utilization of inorganic and organic
753 nutrients, as well as organic carbon. Increased brownification may occur as a result
754 of climate change, and our study points to the need to better understand the negative
755 impacts of tDOM on phytoplankton species in lakes and reservoirs.

756

757 **Acknowledgements**

758 We wish to thank Priyanesh Muhid for bacterial counts, Sian Taylor for chlorophyll
759 analyses and generating graphs, Amanda Neilen for running spectrophotometric
760 analyses, Dale Burford for making mesocosm bags, Seqwater staff, specifically Paul
761 Fisher, Andrew Watkinson, Kate Smolders, and staff at Wyaralong reservoir for
762 assistance with access to reservoir and other logistics, and Queensland Department
763 of Environment and Science Chemistry laboratory for nutrient analyses. This
764 research was supported by funding from the Australian Research Council
765 (LP160100335), Seqwater and Healthy Land and Water.

766

767

768 **References**

- 769 Aguilera, A., Gómez, E.B., Kaštovský, J., Echenique, R.O., Salerno, G.L., 2018. The
770 polyphasic analysis of two native Raphidiopsis isolates supports the unification
771 of the genera Raphidiopsis and Cylandrospermopsis (Nostocales,
772 Cyanobacteria). *Phycologia* 57, 130–146.
- 773 American Public Health Association (APHA), 2005. Standard Methods for the
774 Examination of Water and Wastewater., 21st ed. American Public Health
775 Association, Washington, DC.
- 776 Benner, R., Kaiser, K., 2011. Biological and photochemical transformations of amino
777 acids and lignin phenols in riverine dissolved organic matter. *Biogeochemistry*
778 102, 209–222.
- 779 Boland, D., Brooker, M., Chippendale, G., N, H., Hyland, B., Johnson, R., Kleinig, D.,
780 McDonald, M., Turner, J., 2006. Forest Trees of Australia Fifth Edition, CSIRO.
781 CSIRO Publishing, Collingwood, Australia.
- 782 Burford, M.A., Beardall, J., Willis, A., Orr, P.T., Magalhaes, V.F., Rangel, L.M.,
783 Azevedo, S.M.F.O.E., Neilan, B.A., 2016. Understanding the winning strategies
784 used by the bloom-forming cyanobacterium *Cylandrospermopsis raciborskii*.
785 *Harmful Algae* 54, 44–53.
- 786 Burford, M.A., Davis, T.W., Orr, P.T., Sinha, R., Willis, A., Neilan, B.A., 2014.
787 Nutrient-related changes in the toxicity of field blooms of the cyanobacterium,
788 *Cylandrospermopsis raciborskii*. *FEMS Microbiol. Ecol.* 89.
- 789 Caldero-Pascual, M., Dilvin, Y., Metin, M., Fiorentin, C., Rene, M., Mccarthy, V.,
790 Jeppesen, E., Ali, K., Meryem, G., 2021. The importance of allochthonous
791 organic matter quality when investigating pulse disturbance events in freshwater
792 lakes : a mesocosm experiment. *Hydrobiologia*.
- 793 Caplanne, S., Laurion, I., 2008. Effect of chromophoric dissolved organic matter on
794 epilimnetic stratification in lakes. *Aquat. Sci.* 70, 123–133.
- 795 Chen, F., Lu, J.R., Binder, B.J., Liu, Y.C., Hodson, R.E., 2001. Application of digital
796 image analysis and flow cytometry to enumerate marine viruses stained with
797 SYBR Gold. *Appl. Environ. Microbiol.* 67, 539–545.
- 798 Creed, I.F., Bergström, A.K., Trick, C.G., Grimm, N.B., Hessen, D.O., Karlsson, J.,
799 Kidd, K.A., Kritzberg, E., McKnight, D.M., Freeman, E.C., Senar, O.E.,
800 Andersson, A., Ask, J., Berggren, M., Cherif, M., Giesler, R., Hotchkiss, E.R.,
801 Kortelainen, P., Palta, M.M., Vrede, T., Weyhenmeyer, G.A., 2018. Global
802 change-driven effects on dissolved organic matter composition: Implications for
803 food webs of northern lakes. *Glob. Chang. Biol.* 24, 3692–3714.
- 804 Deininger, A., Faithfull, C.L., Bergström, A.K., 2017. Phytoplankton response to
805 whole lake inorganic N fertilization along a gradient in dissolved organic carbon.
806 *Ecology* 98, 982–994.
- 807 Ekvall, M.K., de la Calle Martin, J., Faassen, E.J., Gustafsson, S., Lürding, M.,
808 Hansson, L.A., 2013. Synergistic and species-specific effects of climate change
809 and water colour on cyanobacterial toxicity and bloom formation. *Freshw. Biol.*
810 58, 2414–2422.
- 811 Fee, E.J., Hecky, R.E., Kasian, S.E.M., Cruikshank, D.R., 1996. Physical and chemical

- 812 responses of lakes and streams. *Limnol. Oceanogr.* 41, 912–920.
- 813 Franklin, H.M., Chen, C.R., Carroll, A.R., Maxwell, P., Burford, M.A., 2020. Plant
814 source and soil interact to determine characteristics of dissolved organic matter
815 leached into waterways from riparian leaf litter. *Sci. Total Environ.* 703, 134530.
- 816 Franklin, H.M., Doederer, K., Neale, P.A., Hayton, J.B., Fisher, P., Maxwell, P.,
817 Carroll, A.R., Burford, M.A., Leusch, F.D.L., 2021. Terrestrial dissolved organic
818 matter source affects disinfection by-product formation during water treatment
819 and subsequent toxicity. *Environ. Pollut.* 283, 117232.
- 820 Graeber, D., Tenzin, Y., Stutter, M., Weigelhofer, G., Shatwell, T., von Tümpling, W.,
821 Tittel, J., Wachholz, A., Borchardt, D., 2021. Bioavailable DOC: reactive nutrient
822 ratios control heterotrophic nutrient assimilation—An experimental proof of the
823 macronutrient-access hypothesis. *Biogeochemistry* 155, 1–20.
- 824 Hamilton, D.P., Wood, S.A., Dietrich, D.R., Puddick, J., 2013. Costs of harmful
825 blooms of freshwater cyanobacteria. *Cyanobacteria An Econ. Perspect.* 245–256.
- 826 Helms, J., Stubbins, A., Ritchie, J., Minor, E.C., 2008. Absorption spectral slopes
827 and slope ratios as indicators of molecular weight, source, and photobleaching of
828 chromophoric dissolved organic matter. *Limnol. Oceanogr.* 53, 955–969.
- 829 Hillebrand H, C-D, D., D, K., U, P., T, Z., 1999. Biovolume calculation for pelagic and
830 benthic microalgae. *J. Phycol.* 35, 403–424.
- 831 Hosomi, M., Sudo, R., 1986. Simultaneous determination of total nitrogen and total
832 phosphorus in freshwater samples using persulfate digestion. *Int. J. Environ.*
833 *Stud.* 27, 267–275.
- 834 Isles, P.D.F., 2020. The misuse of ratios in ecological stoichiometry. *Ecology* 101.
- 835 Isles, P.D.F., Creed, I.F., Jonsson, A., Bergström, A.K., 2021. Trade-offs Between
836 Light and Nutrient Availability Across Gradients of Dissolved Organic Carbon
837 Lead to Spatially and Temporally Variable Responses of Lake Phytoplankton
838 Biomass to Browning. *Ecosystems*.
- 839 Jeffrey, S., Welshmeyer, N., 1997. Spectrophotometric and fluorometric equations in
840 common use in oceanography. In: *Phytoplankton Pigments in Oceanography*
841 (Monographs on Oceanographic Methodology). UNESCO Publication, pp. 597–
842 615.
- 843 Kanerva, S., Kitunen, V., Loponen, J., 2008. Phenolic compounds and terpenes in
844 soil organic horizon layers under silver birch , Norway spruce and Scots pine.
845 *Biol Fertil Soils* 44, 547–556.
- 846 Karlsson, J., Bergström, A.-K., Byström, P., Gudasz, C., Rodríguez, P., Hein, C., 2015.
847 in lake ecosystems R eports R eports. *Ecology* 96, 2870–2876.
- 848 Laue, P., Bährs, H., Chakrabarti, S., Steinberg, C.E.W., 2014. Natural xenobiotics to
849 prevent cyanobacterial and algal growth in freshwater: Contrasting efficacy of
850 tannic acid, gallic acid, and gramine. *Chemosphere* 104, 212–220.
- 851 Lebet, K., Langenheder, S., Colinas, N., Östman, Ö., Lindström, E.S., 2018.
852 Increased water colour affects freshwater plankton communities in a mesocosm
853 study. *Aquat. Microb. Ecol.* 81, 1–17.
- 854 Mackay, E.B., Feuchtmayr, H., De Ville, M.M., Thackeray, S.J., Callaghan, N.,
855 Marshall, M., Rhodes, G., Yates, C.A., Johnes, P.J., Maberly, S.C., 2020.

- 856 Dissolved organic nutrient uptake by riverine phytoplankton varies along a
857 gradient of nutrient enrichment. *Sci. Total Environ.* 722, 137837.
- 858 Matthijs, H.C.P., Jančula, D., Visser, P.M., Maršálek, B., 2016. Existing and emerging
859 cyanocidal compounds: new perspectives for cyanobacterial bloom mitigation.
860 *Aquat. Ecol.* 50, 443–460.
- 861 McDonald, S., Bishop, A.G., Prenzler, P.D., Robards, K., 2004. Analytical chemistry
862 of freshwater humic substances. *Anal. Chim. Acta* 527, 105–124.
- 863 Meyer, N., Bigalke, A., Kaulfuß, A., Pohnert, G., Jena, D., Planck, M., Ecology, C.,
864 Kn, H., Jena, D., 2017. Strategies and ecological roles of algicidal bacteria.
865 *FEMS Microbiol. Rev.* 41, 880–899.
- 866 Monteith, D.T., Stoddard, J.L., Evans, C.D., De Wit, H.A., Forsius, M., Høgåsen, T.,
867 Wilander, A., Skjelkvåle, B.L., Jeffries, D.S., Vuorenmaa, J., Keller, B., Kopécek,
868 J., Vesely, J., 2007. Dissolved organic carbon trends resulting from changes in
869 atmospheric deposition chemistry. *Nature* 450, 537–540.
- 870 Muellner, M.G., Wagner, E.D., Mccalla, K., Richardson, S.D., Woo, Y.T., Plewa, M.J.,
871 2007. Haloacetonitriles vs. regulated haloacetic acids: Are nitrogen-containing
872 DBFs more toxic? *Environ. Sci. Technol.* 41, 645–651.
- 873 Muhid, P., Davis, T.W., Bunn, S.E., Burford, M.A., 2013. Effects of inorganic
874 nutrients in recycled water on freshwater phytoplankton biomass and
875 composition. *Water Res.* 47.
- 876 Nagai, T., Imai, A., Matsushige, K., Fukushima, T., 2006. Effect of iron complexation
877 with dissolved organic matter on the growth of cyanobacteria in a eutrophic
878 lake. *Aquat. Microb. Ecol.* 44, 231–239.
- 879 Neilen, Amanda D, Carroll, A.R., Hawker, D.W., Brien, K.R.O., Burford, M.A., 2019.
880 Effects of photochemical and microbiological changes in terrestrial dissolved
881 organic matter on its chemical characteristics and phytotoxicity towards
882 cyanobacteria. *Sci. Total Environ.* 695, 133901.
- 883 Neilen, A.D., Carroll, A.R., Hawker, D.W., O'Brien, K.R., Burford, M.A., 2019. Effects
884 of photochemical and microbiological changes in terrestrial dissolved organic
885 matter on its chemical characteristics and phytotoxicity towards cyanobacteria.
886 *Sci. Total Environ.* 695.
- 887 Neilen, A.D., Carroll, A.R., Hawker, D.W., O'Brien, K.R., Burford, M.A., 2020.
888 Identification of compounds from terrestrial dissolved organic matter toxic to
889 cyanobacteria. *Sci. Total Environ.* 749, 141482.
- 890 Neilen, A.D., Hawker, D.W., O'Brien, K.R., Burford, M.A., 2017. Phytotoxic effects of
891 terrestrial dissolved organic matter on a freshwater cyanobacteria and green
892 algae species is affected by plant source and DOM chemical composition.
893 *Chemosphere* 184, 969–980.
- 894 O'Brien, K.R., Burford, M.A., Brookes, J.D., 2009. Effects of light history on primary
895 productivity in a phytoplankton community dominated by the toxic
896 cyanobacterium *Cylindrospermopsis raciborskii*. *Freshw. Biol.* 54, 272–282.
- 897 O'Neil, J.M., Davis, T.W., Burford, M.A., Gobler, C.J., 2012. The rise of harmful
898 cyanobacteria blooms: The potential roles of eutrophication and climate change.
899 *Harmful Algae* 14.
- 900 O'Neil, J. M., Davis, T.W., Burford, M.A., Gobler, C.J., 2012. The rise of harmful

- 901 cyanobacteria blooms: The potential roles of eutrophication and climate change.
902 *Harmful Algae* 14, 313–334.
- 903 Park, M.H., Han, M.S., Ahn, C.Y., Kim, H.S., Yoon, B.D., Oh, H.M., 2006. Growth
904 inhibition of bloom-forming cyanobacterium *Microcystis aeruginosa* by rice
905 straw extract. *Lett. Appl. Microbiol.* 43, 307–312.
- 906 Pilla, R.M., Williamson, C.E., Zhang, J., Smyth, R.L., Lenters, J.D., Brentrup, J.A.,
907 Knoll, L.B., Fisher, T.J., 2018. Browning-Related Decreases in Water
908 Transparency Lead to Long-Term Increases in Surface Water Temperature and
909 Thermal Stratification in Two Small Lakes. *J. Geophys. Res. Biogeosciences* 123,
910 1651–1665.
- 911 Prairie, Y.T., 2008. Carbocentric limnology: Looking back, looking forward. *Can. J.*
912 *Fish. Aquat. Sci.* 65, 543–548.
- 913 Redfield, A.C., 1958. The biological control of chemical factors in the environment.
914 *Am. Sci.*
- 915 Seekell, D.A., Lapierre, J.F., Ask, J., Bergstrom, A.K., Deiningner, A., Rodriguez, P.,
916 Karlsson, J., 2015. The influence of dissolved organic carbon on primary
917 production in northern lakes. *Limnol. Oceanogr.* 60, 1276–1285.
- 918 Senar, O.E., Creed, I.F., Trick, C.G., 2021. Lake browning may fuel phytoplankton
919 biomass and trigger shifts in phytoplankton communities in temperate lakes.
920 *Aquat. Sci.* 83, 1–15.
- 921 Seymour, J.R., Amin, S.A., Raina, J.B., Stocker, R., 2017. Zooming in on the
922 phycosphere: The ecological interface for phytoplankton-bacteria relationships.
923 *Nat. Microbiol.* 2.
- 924 Singh, H.P., Mittal, S., Kaur, S., Batish, D.R., Kohli, R.K., 2009. Characterization and
925 antioxidant activity of essential oils from fresh and decaying leaves of
926 *Eucalyptus tereticornis*. *J. Agric. Food Chem.* 57, 6962–6966.
- 927 Solomon, C.T., Jones, S.E., Weidel, B.C., Buffam, I., Fork, M.L., Karlsson, J., Larsen,
928 S., Lennon, J.T., Read, J.S., Sadro, S., Saros, J.E., 2015. Ecosystem
929 Consequences of Changing Inputs of Terrestrial Dissolved Organic Matter to
930 Lakes: Current Knowledge and Future Challenges. *Ecosystems* 18, 376–389.
- 931 Stadler, M., Ejarque, E., Kainz, M.J., 2020. In-lake transformations of dissolved
932 organic matter composition in a subalpine lake do not change its
933 biodegradability. *Limnol. Oceanogr.* 65, 1554–1572.
- 934 Steinberg, C.E.W., Kamara, S., Prokhotskaya, V.Y., Manusadžianas, L., Karasyova,
935 T.A., Timofeyev, M.A., Jie, Z., Paul, A., Meinelt, T., Farjalla, V.F., Matsuo,
936 A.Y.O., Burnison, B.K., Menzel, R., 2006. Dissolved humic substances -
937 Ecological driving forces from the individual to the ecosystem level? *Freshw.*
938 *Biol.* 51, 1189–1210.
- 939 Stetler, J.T., Knoll, L.B., Driscoll, C.T., Rose, K.C., 2021. Lake browning generates a
940 spatiotemporal mismatch between dissolved organic carbon and limiting
941 nutrients.
- 942 Urrutia-Cordero, P., Ekvall, M.K., Ratcovich, J., Soares, M., Wilken, S., Zhang, H.,
943 Hansson, L.A., 2017. Phytoplankton diversity loss along a gradient of future
944 warming and brownification in freshwater mesocosms. *Freshw. Biol.* 62, 1869–
945 1878.

- 946 Williamson, C.E., Stemberger, R.S., Morris, D.P., Frost, T.M., Paulsen, S.G., 1996.
947 Ultraviolet radiation in North American lakes: Attenuation estimates from DOC
948 measurements and implications for plankton communities. *Limnol. Oceanogr.*
949 41, 1024–1034.
- 950 Willis, A., Posselt, A.J., Burford, M.A., 2017. Variations in carbon-to-phosphorus
951 ratios of two Australian strains of *Cylindrospermopsis raciborskii*. *Eur. J.*
952 *Phycol.* 00, 1–8.
- 953 Woelkerling WJ, RR, K., SB, G., 1976. Sedgwick-rafter cell counts: a procedural
954 analysis. *Hydrobiologia* 48, 95–107.
- 955 Xenopoulos, M.A., Barnes, R.T., Boodoo, K.S., Butman, D., Catalán, N., D’Amario,
956 S.C., Fasching, C., Kothawala, D.N., Pisani, O., Solomon, C.T., Spencer, R.G.M.,
957 Williams, C.J., Wilson, H.F., 2021. How humans alter dissolved organic matter
958 composition in freshwater: relevance for the Earth’s biogeochemistry.
959 *Biogeochemistry* 154, 323–348.
- 960 Xiao, M., Hamilton, D.P., Chuang, A., Burford, M.A., 2020. Intra-population strain
961 variation in phosphorus storage strategies of the freshwater cyanobacterium
962 *Raphidiopsis raciborskii*. *FEMS Microbiol. Ecol.* 96, 1–13.
- 963 Xiao, M., Willis, A., Burford, M.A., 2017. Differences in cyanobacterial strain
964 responses to light and temperature reflect species plasticity. *Harmful Algae* 62,
965 84–93.
- 966 Yamashita, Y., Maie, N., Briceño, H., Jaffé, R., 2010. Optical characterization of
967 dissolved organic matter in tropical rivers of the Guayana Shield, Venezuela. *J.*
968 *Geophys. Res. Biogeosciences* 115.
- 969

970 **Supplementary Information**

971

972 S1: Identification of compounds in concentrated *Eucalyptus* leachate

973 Approximately 4 g of the crude *Eucalyptus* leachate was obtained, and a 37 mg
974 aliquot was dissolved in DMSO-*d*₆ to obtain 1D and 2D NMR. Due to the complexity
975 of this ¹H NMR data (overlapping peaks), the extract was fractionated by HPLC.
976 Using a Merck Hitachi HPLC system equipped with a L-7100 pump, a L-7455 PDA
977 detector and a D-7000 data interface, fractions were collected using a Gilson 215
978 liquid handler. An aliquot (870.0 mg) of *Eucalyptus* leachate that was used in the
979 mesocosm experiments was pre-absorbed onto C₁₈ silica gel (1 g) and loaded into a
980 refillable guard column (20 mm x 10 mm). As the sample was a water extract and
981 therefore likely to contain a large mass of matter that did not bind to the C₁₈, the
982 guard column was eluted in 100% H₂O until no coloured material was visible in the
983 eluent. This material (409.0 mg) was dried and 1D and 2D NMR acquired on an
984 aliquot (22.3 mg) of this sample. The remaining sample in the guard column was
985 separated by reverse phase HPLC using a Synergi 4 μm hydro column 80 Å (150 mm
986 x 21.2 mm, 5μm) using a linear gradient from 100% H₂O to 100% MeOH over 60
987 min, fractions were collected every min. ¹H NMR data was acquired on every second
988 HPLC fraction, from fractions 2 to 58. Ten fractions (14, 22, 26, 30, 32, 34, 36, 38, 46
989 and 52) were selected to acquire additional 2D NMR data. Compounds were
990 successfully identified from fraction 14, 22, 26, 30, 32, 34, 36, 38; no compounds
991 were successfully identified from fractions 46 and 52. All NMR analyses was acquired
992 at 25 °C in DMSO-*d*₆, using a 500 MHz Bruker® Avance III HD spectrometer
993 equipped with a BBFO Smartprobe, 5 mm with Z-gradient and automatic tune and
994 match or a 800 MHz Bruker® Avance III HD spectrometer equipped with a 5 mm
995 triple-resonance cryoprobe

Supplementary figures

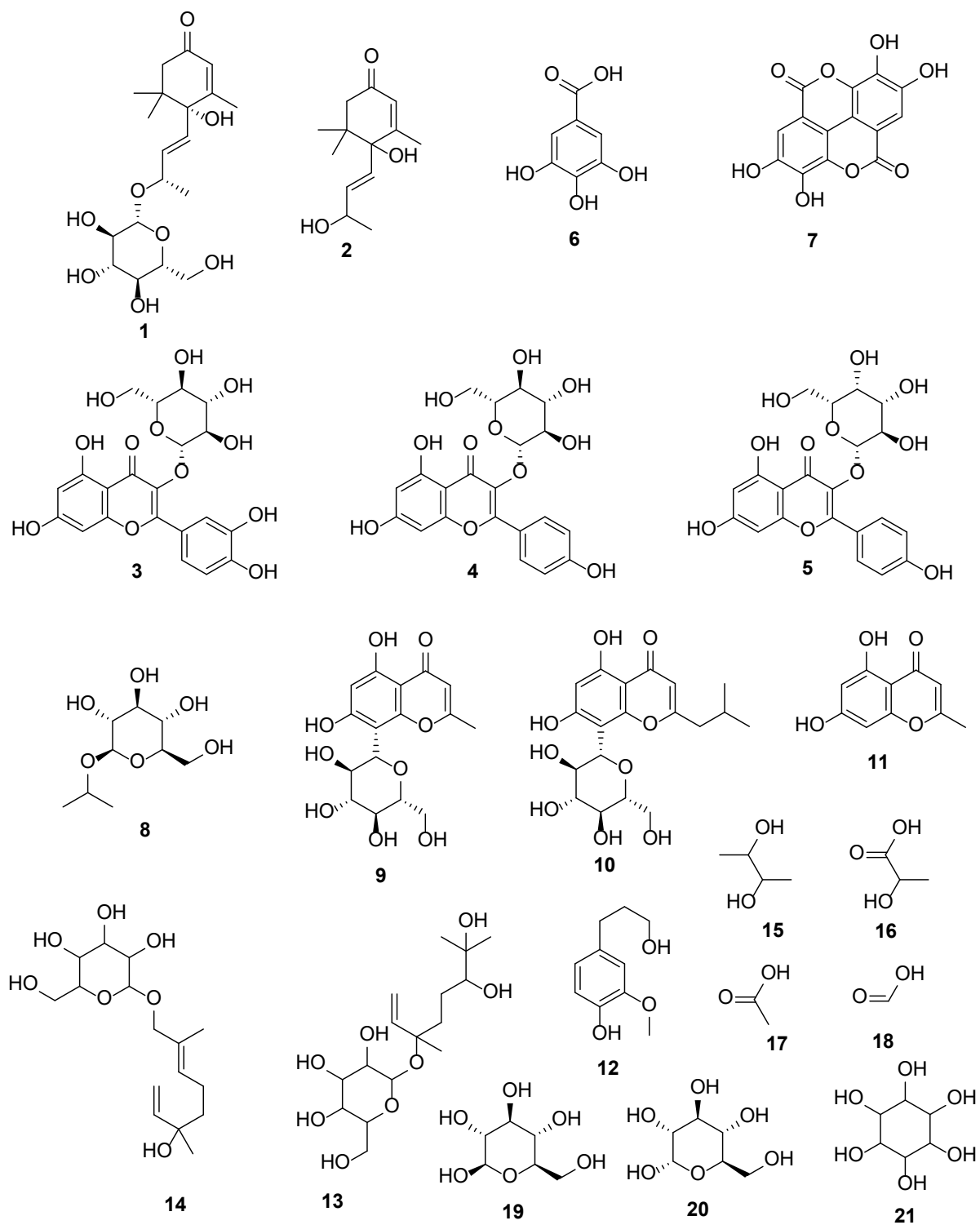


Figure S1. Compounds identified from *Eucalyptus tereticornis*.

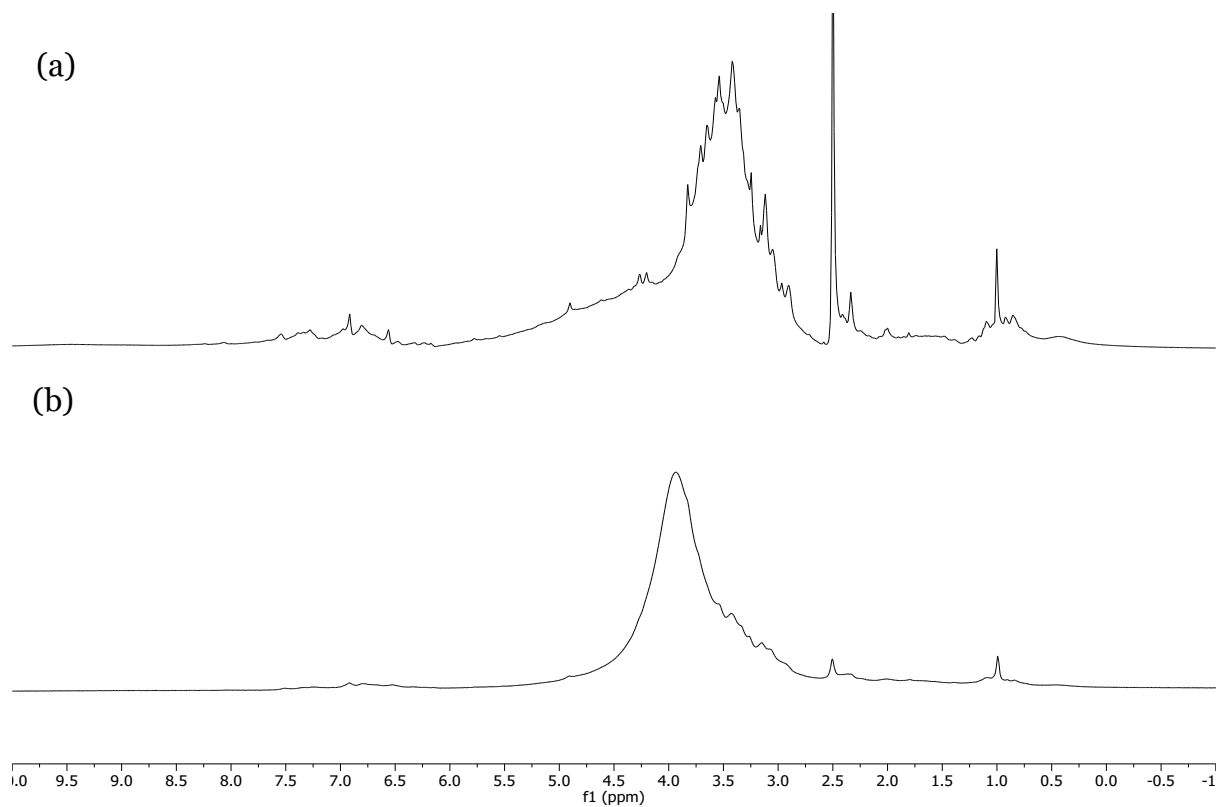


Figure S2. ^1H NMR spectra acquired for (a) the crude/raw extract and (b) the material eluted from the guard column before the HPLC.

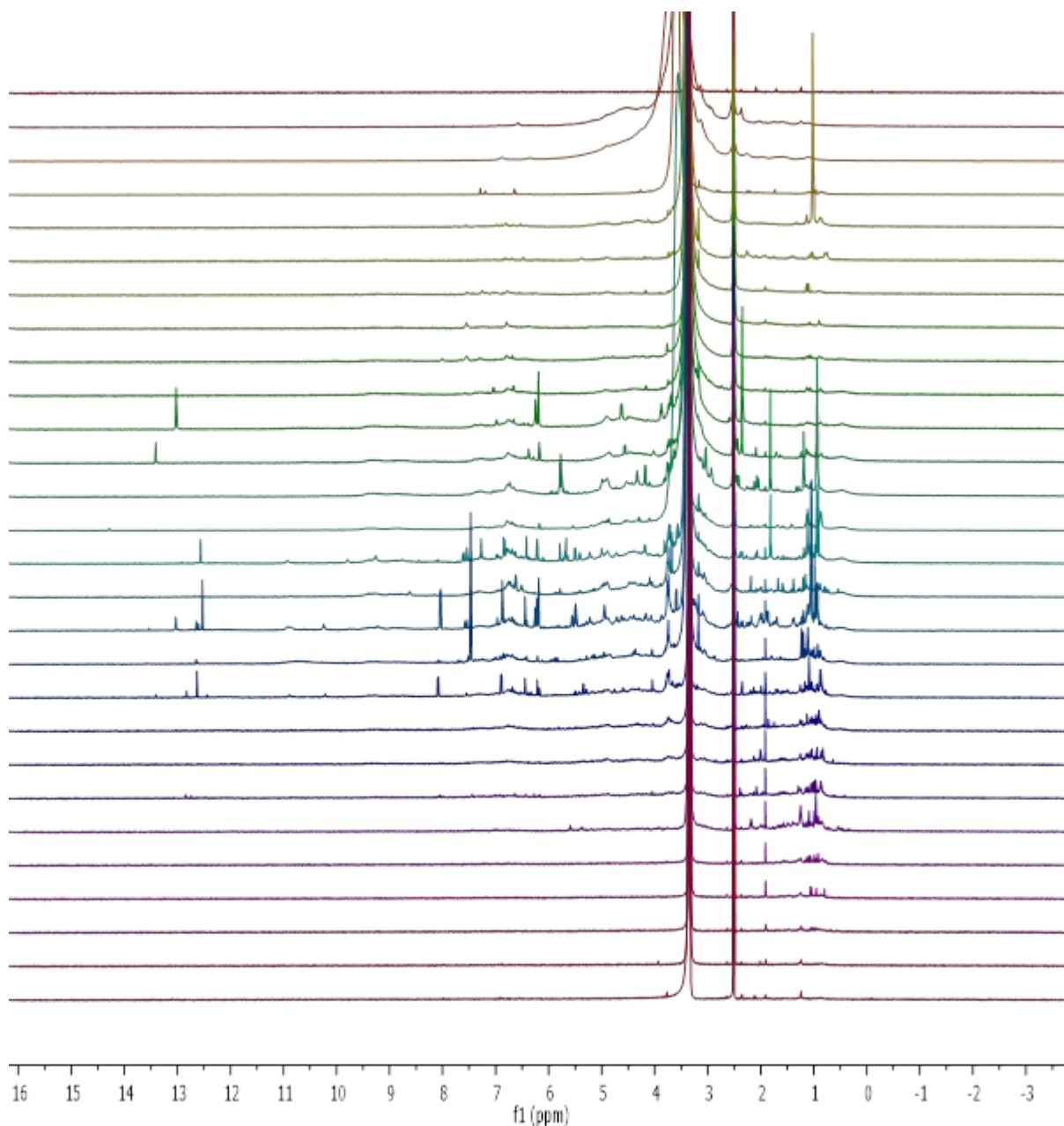


Figure S3. ¹H NMR spectra acquired for every 2nd HPLC fraction from 2 to 58, spectra are arranged in descending order.

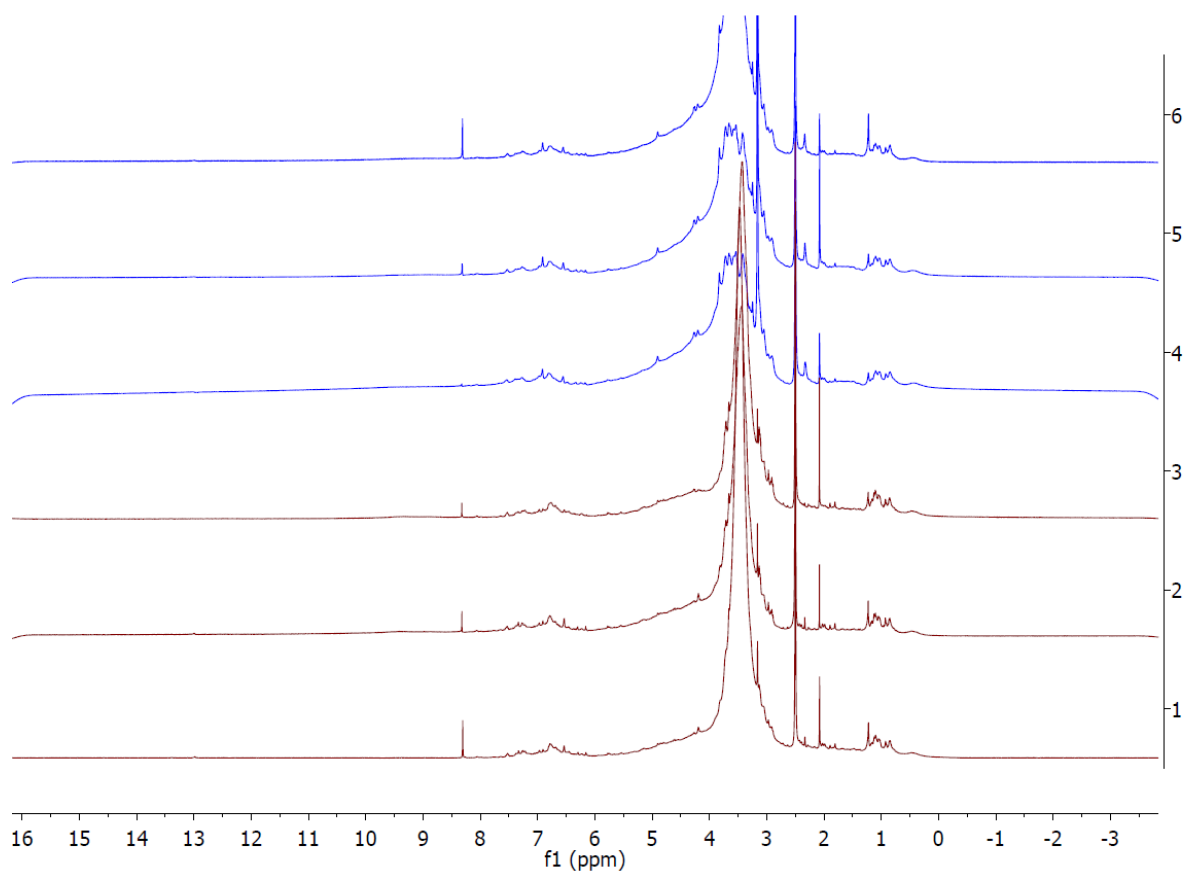


Figure S4: All ^1H NMR spectra for raw *Eucalyptus* leachate (blue) DOM diluted in DI water to 25 mg L^{-1} and leachate that has been aged (Red) in natural light/dark conditions for 5 days.

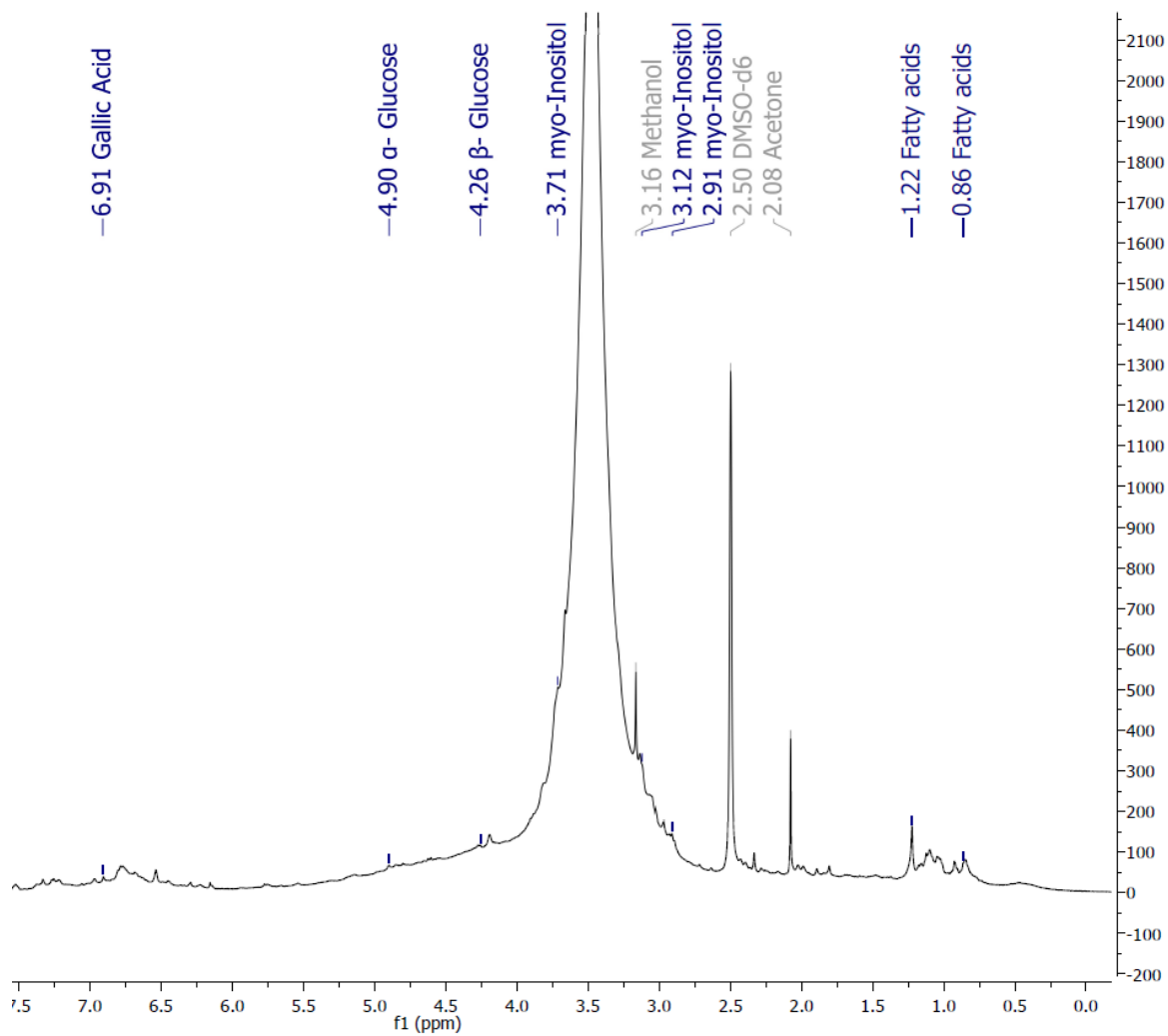


Figure S5: Example showing peaks associated with identified compounds in ¹H NMR spectra from sample of *Eucalyptus* leachate DOM diluted in DI water to 25 mg L⁻¹ DOC and aged in natural light/dark conditions for 5 days.

Supplementary tables

Table S1. The fraction from which each compound was identified from the *Eucalyptus* leaf leachate, the name(s) and unique CAS number of each of the compounds and references used to confirm the structures of the compounds.

Compound number	Compound Name(s)	CAS number	References
1	(6R,9S)-roseoside corchoinoside C	723334-68-7	https://doi.org/10.1248/cpb.45.464 https://doi.org/10.1248/cpb.53.541
2	vomifoliol	23526-45-6	https://doi.org/10.1002/jccs.20000050
3	quercetin 3-glucoside isoquercetin	482-35-9	https://doi.org/10.1002/mrc.3829 https://bpsa.journals.ekb.eg/article_65468_8e82850c94f5f358b43d5367ff8f7afa.pdf
4	kaemferol 3-glucopyranoside astragaline	480-10-4	https://bpsa.journals.ekb.eg/article_65468_8e82850c94f5f358b43d5367ff8f7afa.pdf
5	kaempferol 3-galactoside	23627-87-4	https://bpsa.journals.ekb.eg/article_65468_8e82850c94f5f358b43d5367ff8f7afa.pdf

6	ellagic acid	476-66-4	
7	gallic acid	149-91-7	
8	1-methylethyl β -D-glucopyranoside	5391-17-3	https://pubs.acs.org/doi/pdf/10.1021/ja00479a014
9	isobiflorin	152041-16-2	https://doi.org/10.1016/S0031-9422(96)00836-9
10	8- β -C-glucopyranosyl-5,7-dihydroxy-2-isobutylchromone	1359074-70-6	https://doi.org/10.1002/cbdv.201100021
11	noreugenin	1013-69-0	https://doi.org/10.1016/0031-9422(90)85130-8
12	dihydroconiferyl alcohol	2305-13-7	https://pubs.acs.org/doi/pdf/10.1021/ja00157a002
13	6,7-dihydroxy-dihydrolinalool-3-O- β -d-glucopyranoside	288152-87-4	https://doi.org/10.1016/S0031-9422(99)00447-1 https://doi.org/10.1016/j.bse.2015.07.010
14	betulalbuside A	64776-96-1	https://doi.org/10.1002/hlca.19930760716
15	2,3-butanediol	513-85-9	
16	2-hydroxypropanoic acid	171664-79-2	
17	acetic acid	64-19-7	
18	formic acid	64-18-6	
19	β -Glucose	492-61-5	
20	α - Glucose	492-62-6	

Table S2: Mean (SD) phytoplankton and bacterial densities (cells mL⁻¹) in each treatment throughout experiment. Significant differences shown as a, b, c, d showing differences between treatments.

	Treat ment	<i>R.raciborskii</i>	Cyanobacteria	Chlorophytes	Bacillariophytes	Bacteria
	DOC (mg L ⁻¹)	Cells mL ⁻¹				
Day 0	AMB	161,917 (31, 164)	330,474 (41.013)	8,988 (1,416)	6000 (668)	
Day 3	AMB					3,273,333 (344,867) ^a
	0					3,245,000 (522,143) ^a
	2					3,457,500 (896,042) ^a
	3.3					3,737,500 (821.356) ^a
	5.9					3,135,000 (1,068,878) ^a
	25					12,992,500 (5,282,950) ^b
Day 5	AMB	122,021 (21,971) ^{ab}	356,553 (62,130) ^{ab}	8,163 (2,186)	5,217 (994) ^{ab}	
	0	165,442 (60,967) ^a	447,909 (109,628) ^a	11,313 (3,328)	7,550 (1,473) ^{ab}	
	2	201,250 (47,177) ^a	526,568 (127,994) ^a	9,475 (5,468)	6,533 (1,548) ^{ab}	
	3.3	53,585 (35,232) ^{ab}	308,755 (68,271) ^{ab}	9,925 (218)	6,257 (2,385) ^{ab}	

	5.9	14,142 (17,175) ^b	113,453 (129,693) ^b	5,500 (3,605)	7,450 (1,276) ^a	
	25	13,445 (9,767) ^b	53,223 (18,092) ^b	4,650 (946)	3,075 (1,237) ^b	
Day 7	AMB	163,167 (15,712) ^{ab}	420,581 (56,229) ^{ab}	4,456 (1,310) ^a	7,850 (1,432) ^{ab}	
	0	221,896 (64,299) ^a	537,629 (93,708) ^a	31,000 (43,661) ^{ab}	10,254 (2,139) ^a	
	2	231,000 (29,606) ^a	664,842 (31,417) ^a	15,344 (5,637) ^b	5,616 (1,146) ^{abc}	
	3.3	86,021 (27,954) ^{abc}	352,844 (23,210) ^{ab}	9,950 (2,025) ^{ab}	4,130 (1,104) ^{bc}	
	5.9	5,188 (2,421) ^c	31,781 (20,481) ^b	4,338 (1,121) ^{ab}	7,242 (638) ^{ab}	
	25	26,040 (16,112) ^{bc}	66,745 (30,709) ^b	6,305 (2,687) ^{ab}	2,803 (585) ^c	
Day 10	AMB	165,833 (20,773)	385,536 (53,302)	3,083 (1,508)	9,175 (612)	
	0	1,975 (742) (24,225 (9,440)	6,638 (2,952)	9,834 (7,967)	
	2	380,667 (197,047)	785,100 (245,602)	8,000 (2,192)	9,225 (1,096)	
	3.3	307,556 (189,726)	791,264 (330,639)	8,150 (4,427)	9,817 (3,467)	
	5.9	230,000	701,930	7,550	3,901	
	25	68,283 (129,376)	223,680 (370,487)	6,240 (1079)	4,870 (1,642)	

Phytoplankton species	Phylum	Day 0	Day 10
<i>Chrysochlorum bergii</i>	Cyanobacteria	2,113 (1547)	788 (295)
<i>C. ovalisporum</i>	Cyanobacteria	2,350 (1493)	1,338 (585)
<i>Raphidiopsis mediterranea</i>	Cyanobacteria	1,325 (1015)	1,033 (503)
<i>R. raciborskii</i>	Cyanobacteria	161,917 (31,165)	165,833 (20,773)
<i>Sphaerospermopsis aphanizomenoides</i>	Cyanobacteria	2,900 (502)	3,463 (1064)
<i>S. reniformes</i> (coiled)	Cyanobacteria	550 (71)	Below detection
<i>Anagnostidinema amphibium</i>	Cyanobacteria	7,288 (2024)	6,300 (1417)
<i>Planktolyngbya limnetica</i>	Cyanobacteria	81,333 (10,708)	97,500 (23,004)
<i>Pseudanabaena limnetica</i>	Cyanobacteria	18,455 (2969)	37,100 (5033)
<i>Anathece</i> spp.	Cyanobacteria	1,238 (585)	19,039 (6231)
<i>Aphanocapsa</i> spp.	Cyanobacteria	5,400 (3778)	46,101 (17,692)
<i>Cyanogranis libera</i>	Cyanobacteria	45,881 (11,844)	7,075 (1514)
<i>Ankistrodesmus</i> spp.	Chlorophyte	8,500 (1322)	2,700 (1322)
<i>Scenedesmus</i> spp.	Chlorophyte	100 (0)	67 (47)
<i>Staurastrum</i> spp.	Chlorophyte	100 (50)	100 (50)
<i>Tetraedron</i> spp.	Chlorophyte	363 (103)	275 (144)
<i>Achnanthes</i> spp.	Bacillariophyte	225 (50)	950 (187)
<i>Synedra</i> spp.	Bacillariophyte	5,775 (714)	8,225 (591)